Chapter 3 Modeling Approaches

- Rigorous coupling wave analysis (RCWA/FMM)
- Finite difference and time domain (FDTD)
- Discrete dipole approximation (DDA)
- Mutiple multipole program (MMP)
- Mie theory
- Beam propagation method

Rigorous Coupling Wave Analysis

Figure 1: J.C. Maxwell and H.R. Hertz

RCWA

- To analyze the response of subwavelength gratings, the vectorial nature of light must be taken into account through a resolution of the Maxwell equation

→ Rigorous Coupled-Wave Analysis (RCWA)
or Fourier Modal Method (FMM)

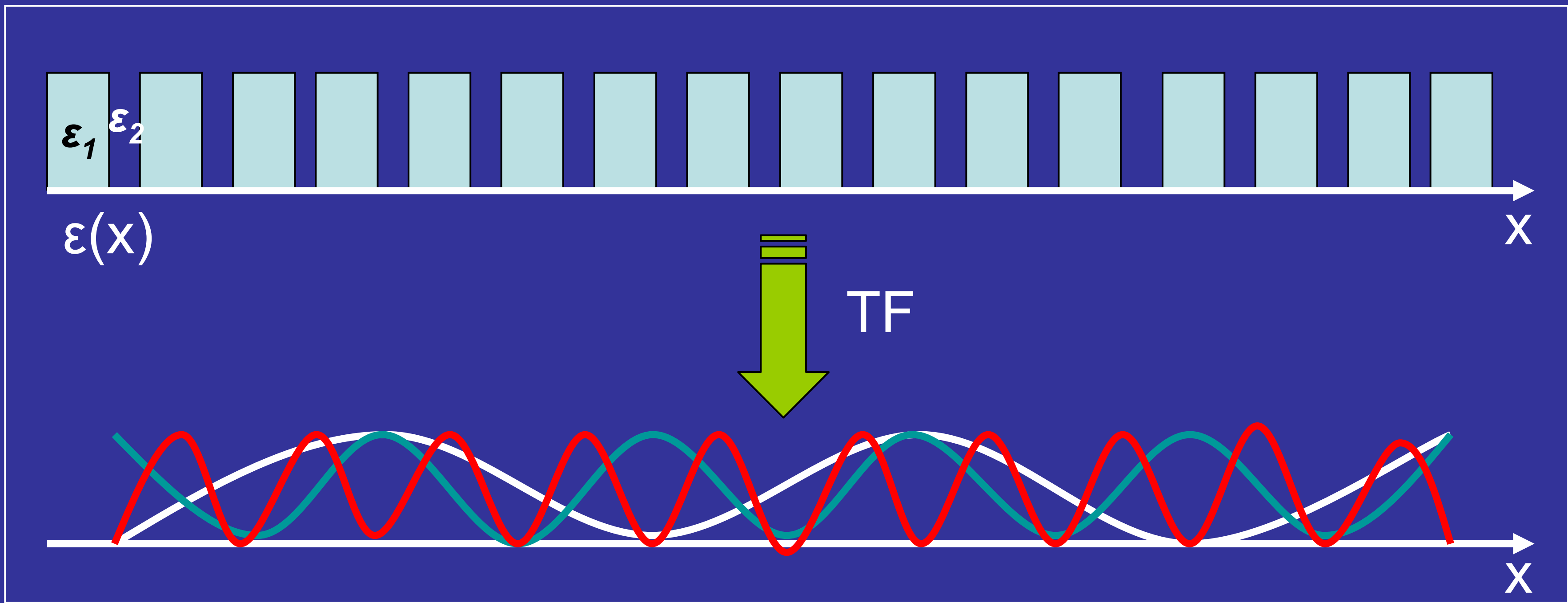

Fields and permittivities are decomposed in a Fourier basis and then matched at the grating layer boundaries to yield the diffraction order complex amplitudes.

Huygen's principle

- Huygen's principle offers an explanation for why and how waves bend (or *diffract*) when passing an obstruction
  - every point on a wave front acts as a source of tiny spherical *wavelets* that travel forward with the same speed as the wave
  - the wave front at a later time is then the linear superposition of all the wavelets

Christian Huygens (1629-1695)

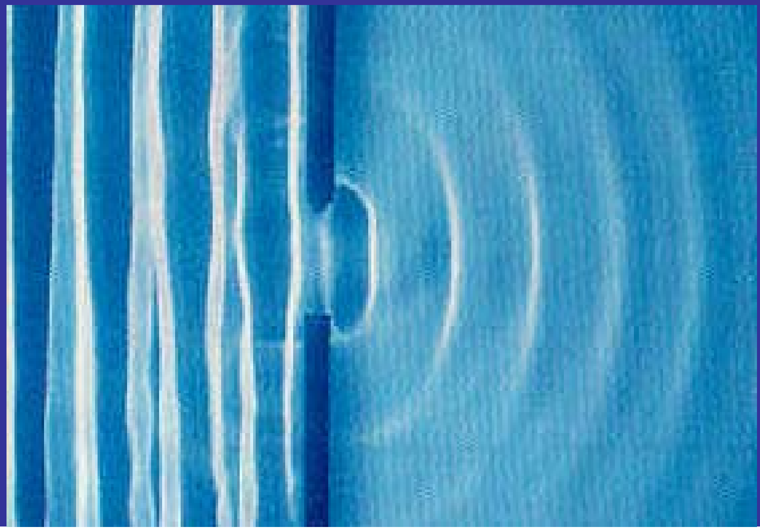

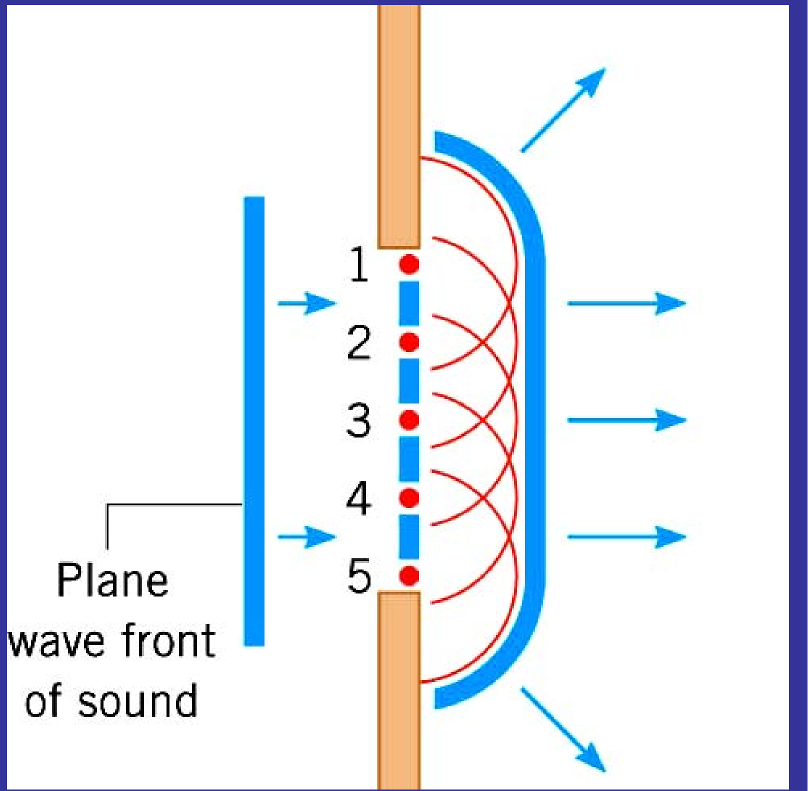

Validity of Scalar Field

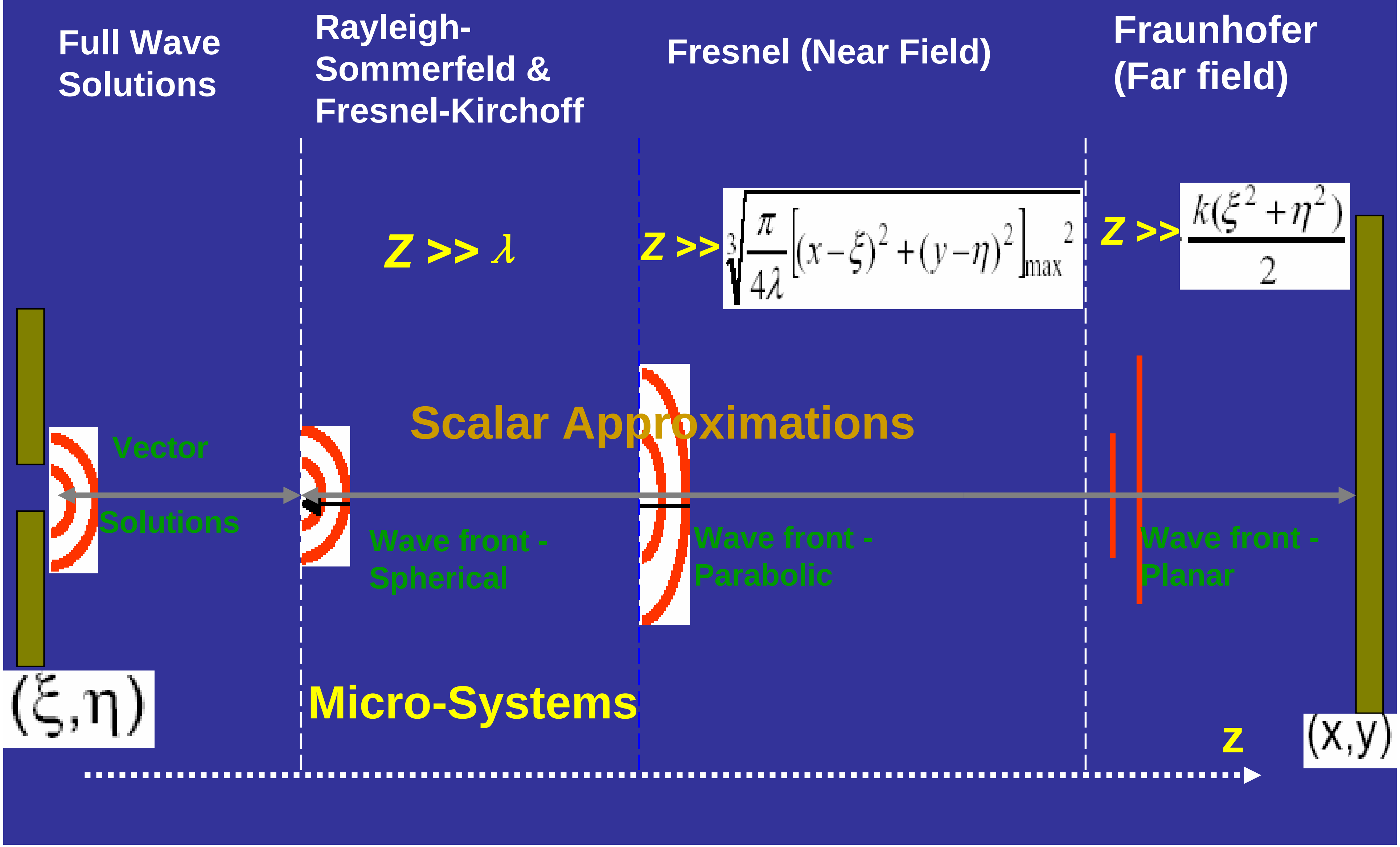

Four basic equations in EM wave

- Helmholtz’s equation
- Green’s function
- Green’s formula
- Kirchhoff’s formuls

a） Helmholtz’s equation

In source free space, EM filed $\vec{E}$和$\vec{B}$ **satisfies**

$$\nabla^2\vec{E}-\frac{1}{\upsilon^2}\frac{\partial^2\vec{E}}{\partial t^2}=0$$

$$\nabla^2\vec{B}-\frac{1}{\upsilon^2}\frac{\partial^2\vec{B}}{\partial t^2}=0$$

Helmholtz’s equation $\nabla^2\psi+K^2\psi=0$

$$k=\omega/v$$

$$\psi(x,y,z,t)=\phi(x,y,z)e^{-i\omega t}$$

b) Green's function

The same as static filed，assume $G(\vec{x},\vec{x}')$ **is Green function of Helmholtz's equation：**

$$G(\vec{x},\vec{x}') = G(x,y,z;x',y',z') = \frac{e^{ikr}}{r}$$

where $r = \left[(x-x')^2 + (y-y')^2 + (x-z')^2\right]^{1/2}$

as

$$\nabla^2 G = \nabla^2 \frac{e^{ikr}}{r}$$

$$= \frac{1}{r}\nabla^2 e^{ikr} + 2(\nabla\frac{1}{r})\cdot(\nabla e^{ikr}) + e^{ikr}\nabla^2\frac{1}{r}$$

and $$\frac{1}{r}\nabla^2 e^{ikr} + 2(\nabla\frac{1}{r})\cdot(\nabla e^{ikr})$$

$$= \frac{1}{r^3}\frac{d}{dr}(r^2\frac{d}{dr}e^{ikr}) - 2(\frac{\vec{r}}{r^3})\cdot(ike^{ikr}\frac{\vec{r}}{r})$$

$$= -k^2\frac{e^{ikr}}{r} = -k^2 G$$

And as $$\nabla^2\frac{1}{r} = \frac{1}{r^2}\frac{d}{dr}(r^2\frac{d}{dr}\frac{1}{r}) = \begin{cases} 0 & 当 r \neq 0 \\ \infty & 当 r = 0 \end{cases}$$

and $\int_V \nabla \frac{1}{r} d\tau = \int_V \nabla \cdot \nabla \frac{1}{r} d\tau = \oiint_S \nabla \frac{1}{r} \cdot d\vec{s}$

$$= -\oiint_S \frac{\vec{r}}{r^3} \cdot d\vec{s} = -\oiint_S d\Omega = -4\pi$$

We obtain: $\nabla^2 G + k^2 G = -4\pi\delta(\vec{x} - \vec{x}')$

Note:

Helmholtz's equation and Green Function:

Same point: they are wave equation

Different: the former is source free equation, and the latter is point source equation.

c) Green's formula

Put G and ψ into Green function，we have

$$\int_V \left[\psi(\vec{x}')\nabla'^2 G(\vec{x}',\vec{x}) - G(\vec{x}',\vec{x})\nabla'^2\psi(\vec{x}')\right] d\tau'$$

$$= \oiint_S \left[\psi(\vec{x}')\nabla' G(\vec{x}',\vec{x}) - G(\vec{x}',\vec{x})\nabla'\psi(\vec{x}')\right]\cdot d\vec{s}$$

where $d\vec{s}$ is area unit with vector from V *to inside*，if $\hat{\vec{n}}$ is normal direction in V，then

$$d\vec{s}' = -\hat{\vec{n}}\,ds'$$

Above equation change to：

$$\int_V \left[\psi(\vec{x}\,')\nabla'^2 G(\vec{x}\,',\vec{x}) - G(\vec{x}\,',\vec{x})\nabla'^2\psi(\vec{x}\,')\right] d\tau'$$

$$= \oiint_S \left[G(\vec{x}\,',\vec{x})\nabla'\psi(\vec{x}\,') - \psi(\vec{x}\,')\nabla' G(\vec{x}\,',\vec{x})\right]\cdot \hat{\vec{n}}\, ds'$$

This is Green formular.

d) Kirchhoff's formuls

Regarding G as known parameter which satisfies Green function, it has

$$\nabla^2 G + k^2 G = -4\pi\delta(\vec{x} - \vec{x}\,')$$

because $\nabla' G(\vec{x}'.\vec{x}) = \nabla' \frac{e^{ikr}}{r} = \frac{1}{r}\nabla' e^{ikr} + e^{ikr}\nabla' \frac{1}{r}$

$$= -ikG\frac{\vec{r}}{r} + G\frac{\vec{r}}{r^2}$$

Put into Green function，and obtain

$$\int_V \left\{\psi(\vec{x}')\left[-k^2 G(\vec{x}',\vec{x}) - 4\pi\delta(\vec{x}-\vec{x}')\right] - G(\vec{x}'.\vec{x})\left[-k^2\psi(\vec{x}')\right]\right\} d\tau'$$

$$= \oiint_S \left\{G(\vec{x}',\vec{x})\nabla'\psi(\vec{x}') - \psi(\vec{x}')\left[-ikG(\vec{x}',\vec{x})\frac{\vec{r}}{r} + G(\vec{x}'.\vec{x})\frac{\vec{r}}{r}\right]\right\}\cdot \hat{\vec{n}}ds'$$

The Fourier Modal Method, also known as Rigorous Coupled Wave Analysis (RCWA), is ideally suited to simulating the optical response of 2D, periodic surface relief structures, and most especially binary surfaces. It involves the expansion into spatial Fourier components of the both the dielectric function and the associated fields, followed by a numerical solution of the boundary equations. The approach can yield both reflected and transmitted complex diffraction efficiencies, as well the associated field distributions both inside and outside the structure.

Calculation examples

- ✓ single metallic slit
- ✓ Metallic slit with corrugated grooves
- ✓ Combination of SPP and photonic crystal
- ✓ micro-Fresnel lenses
- ✓ Metallic nanoparticles
- ✓ Nanophotonic structures
- ✓ Double slits diffraction with width tuning

RCWA is also called Fourier Modal Method

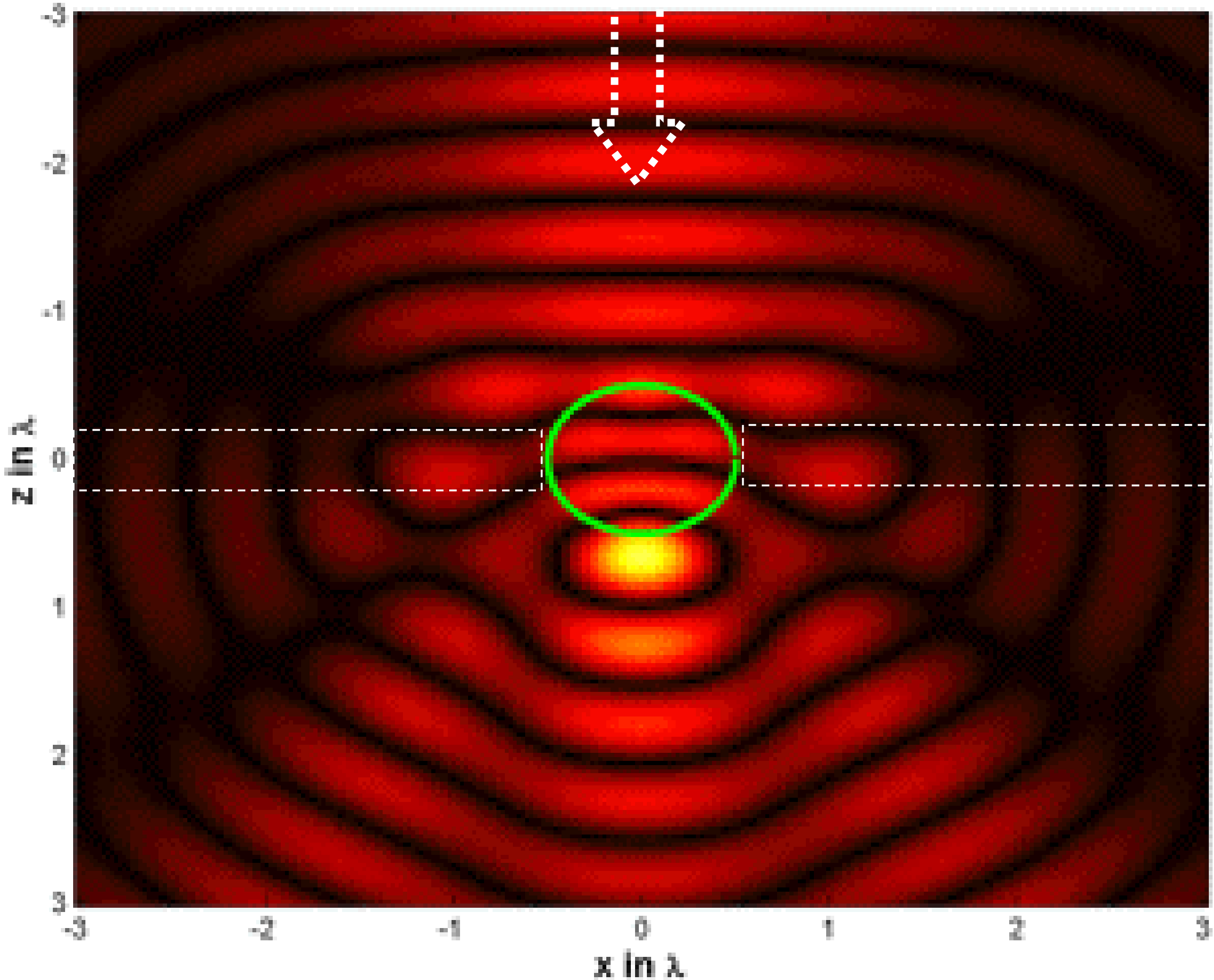

Figure 2: Diffraction of a Gaussian beam by a glass cylinder

Interaction of a plan wave with a slit-on-glass aperture. The plane wave is incident from the bottom and has a wavelength of 549 nm. The slit is 100 nm wide, the Cr layer is 100 nm thick. The left image is TM polarization and the right image TE polarization.

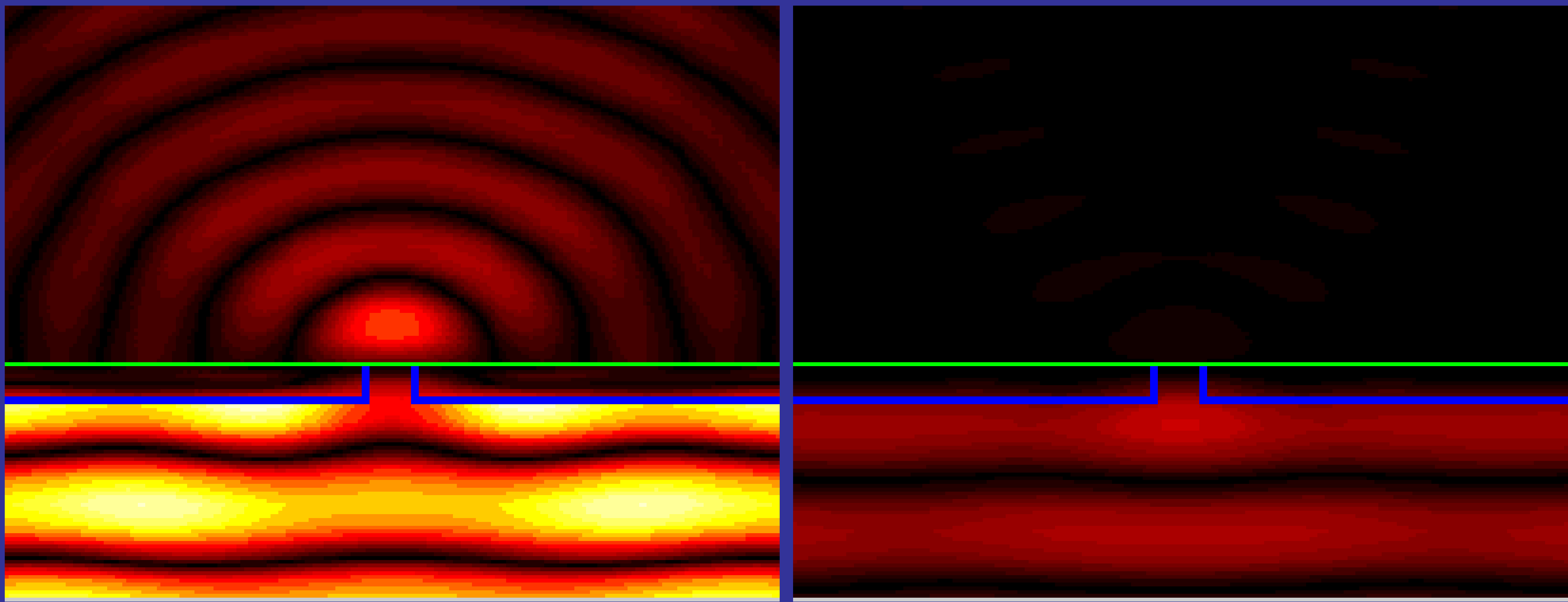

TM TE

Figure 3: Passage of light through a slit using the FMM

Young's double slit experiment

- In 1801 Thomas Young performed an experiment that irrefutably demonstrated the wave nature of light
  - before this there had been a lot of debate between the particle camp (Newton) and the wave camp (Huygens)

- Monochromatic (single frequency) light is first shone through a single slit
  - this makes the light that passes through the single slit coherent (we can avoid this step today using lasers)

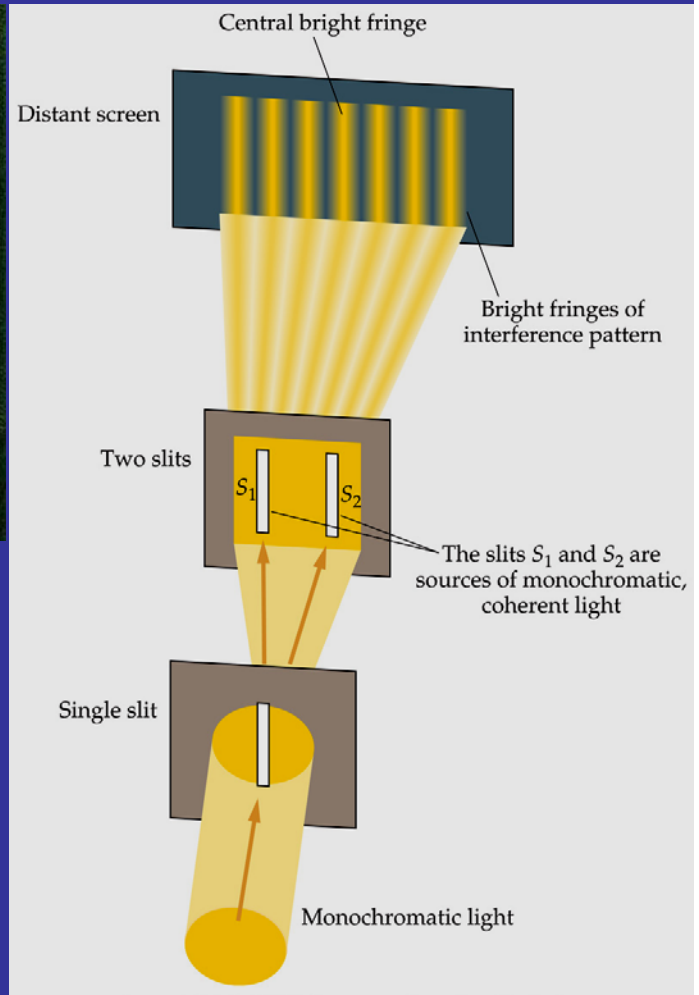

- the light from the single slit is then used to illuminate a double-slit, which produces an interference pattern on a screen behind it

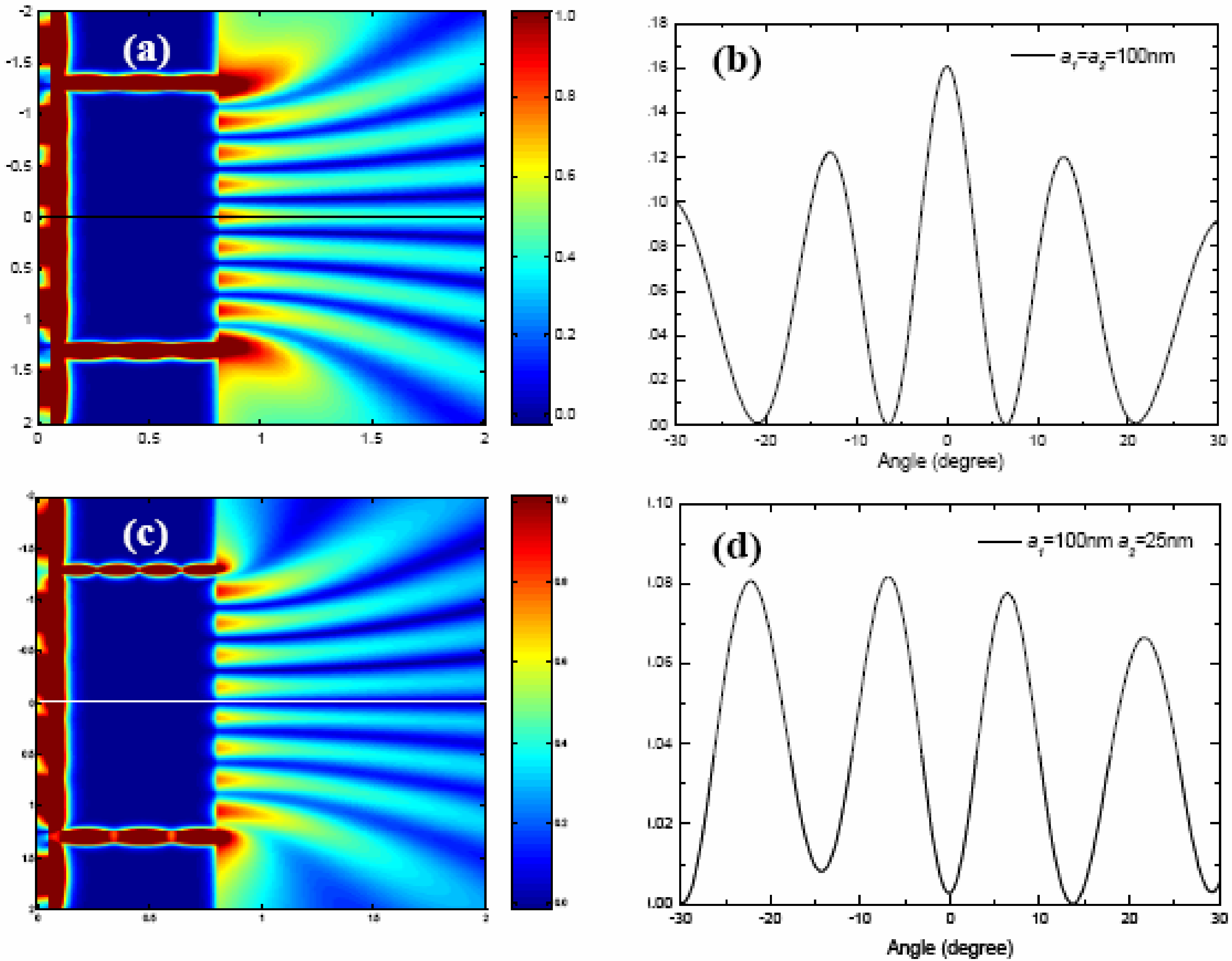
(a)
(b)
a1=a2=100nm
Angle (degree)
(c)
(d)
a1=100nm a2=25nm
Angle (degree)

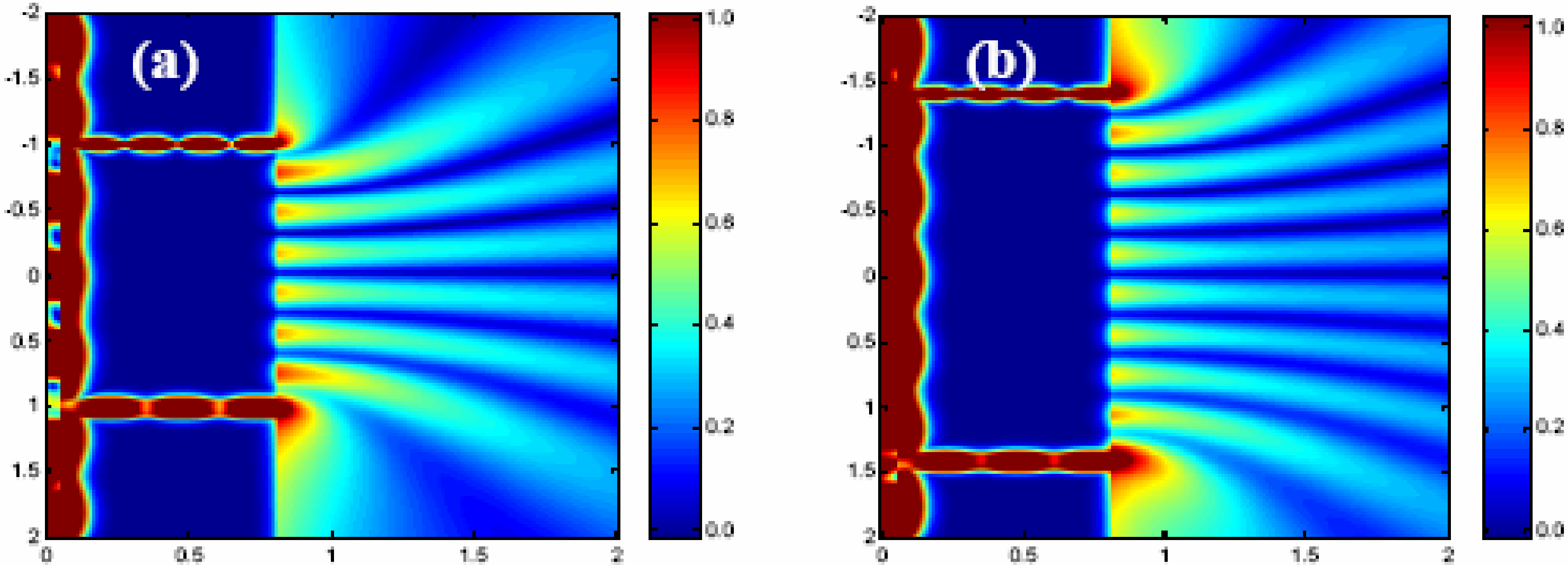

d=2.0μm

d=2.8μm

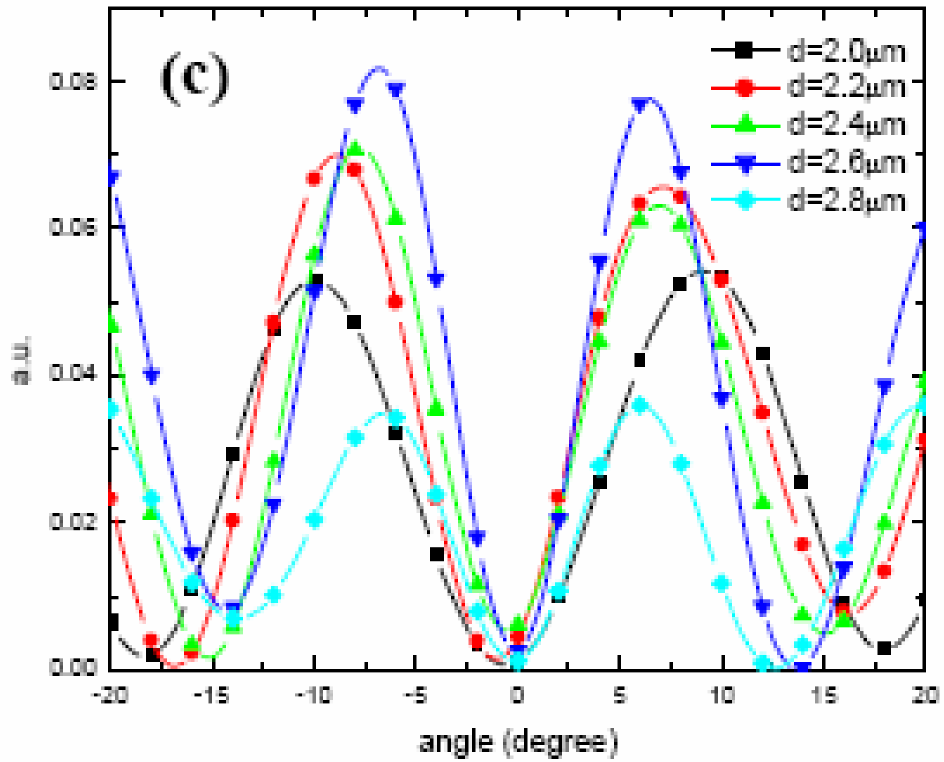

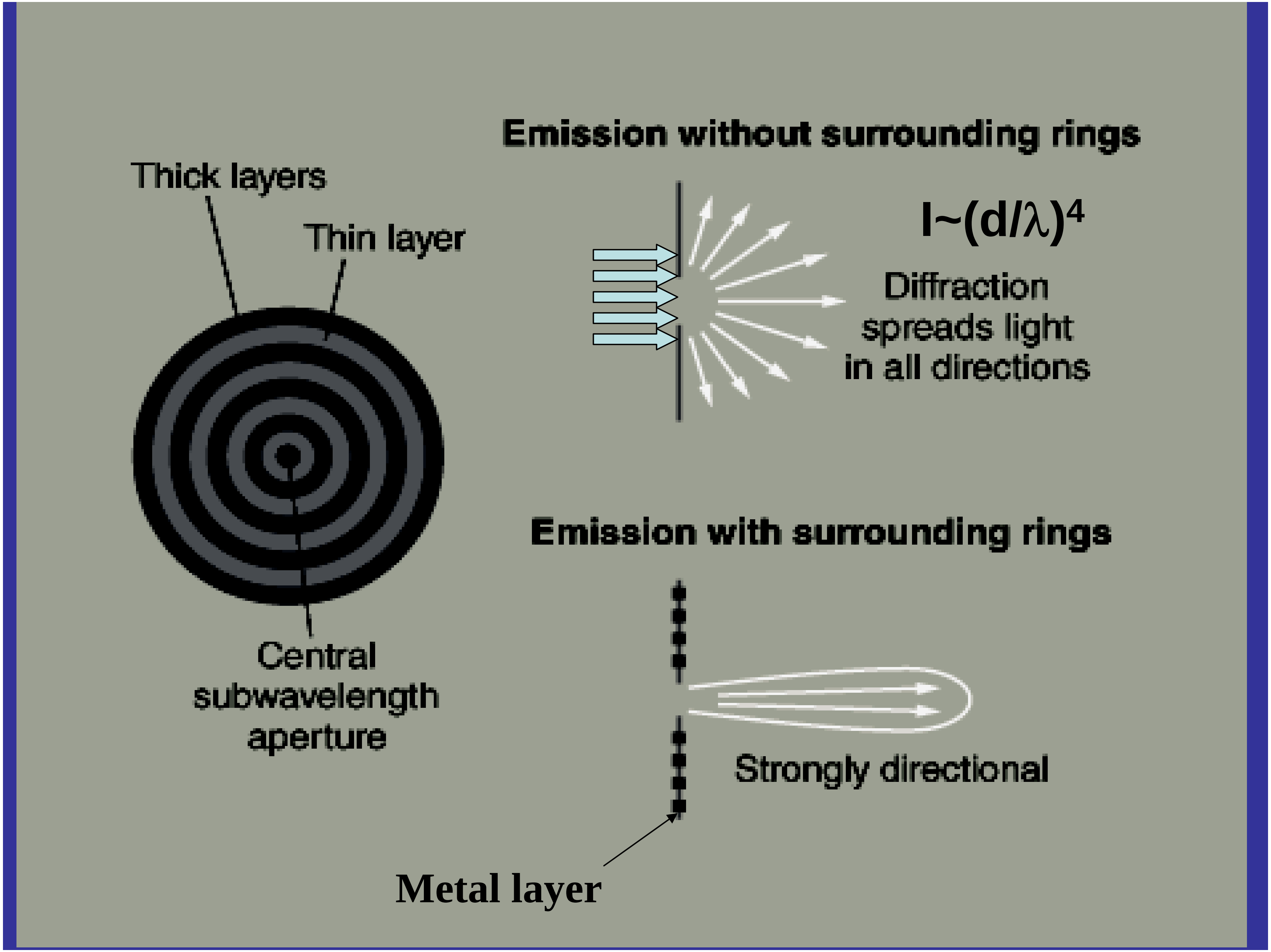

Thick layers
Thin layer
Central subwavelength aperture
Emission without surrounding rings
$I \sim (d/\lambda)^4$
Diffraction spreads light in all directions
Emission with surrounding rings
Strongly directional
Metal layer

Wave optics: diffraction effect

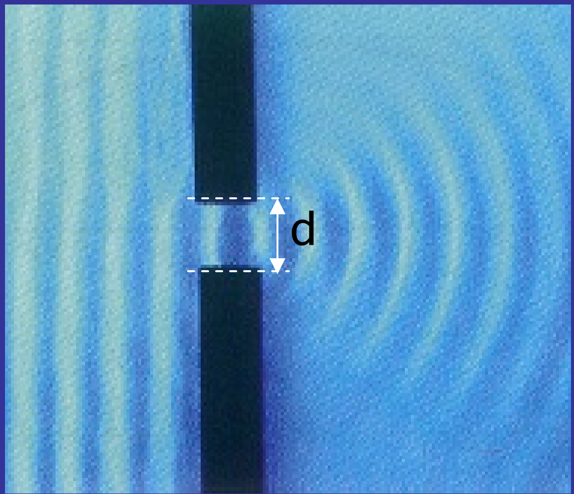

if $\lambda/2 > d$, the transmission through the hole will be strongly suppressed

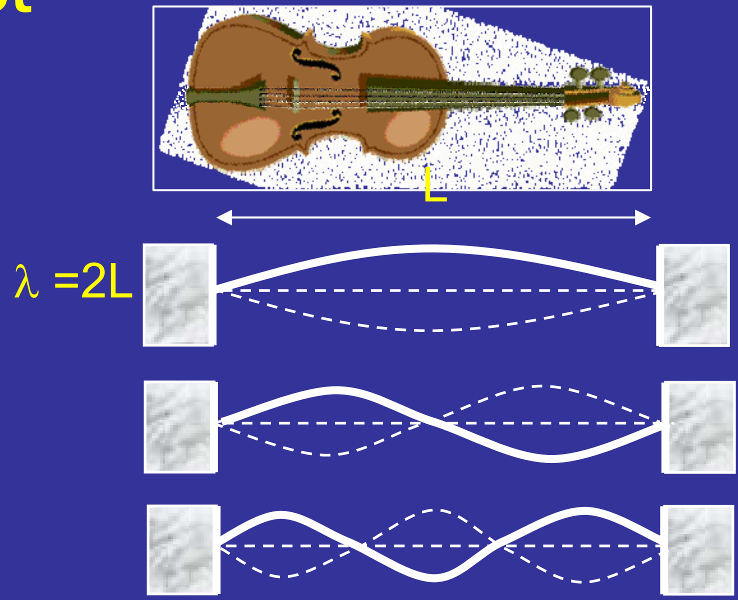

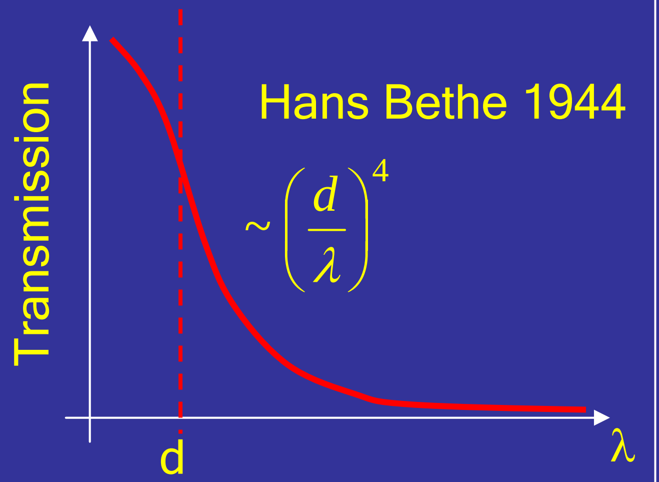

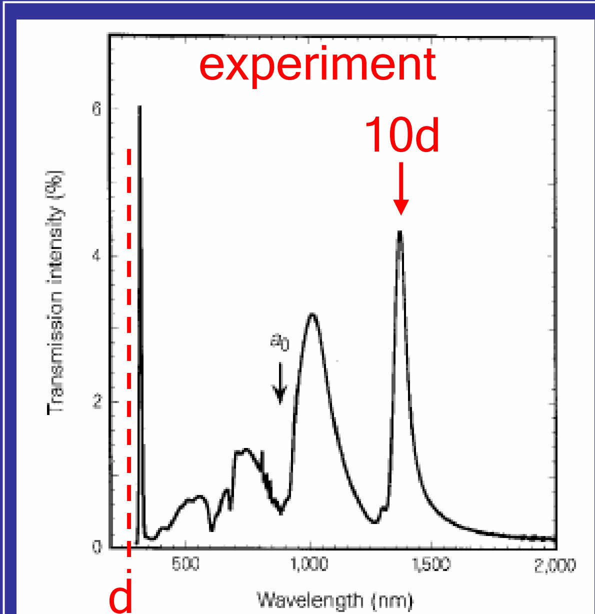

The experimental findings imply that that the array itself is an active element, not just a passive geometrical object in the path of incident light

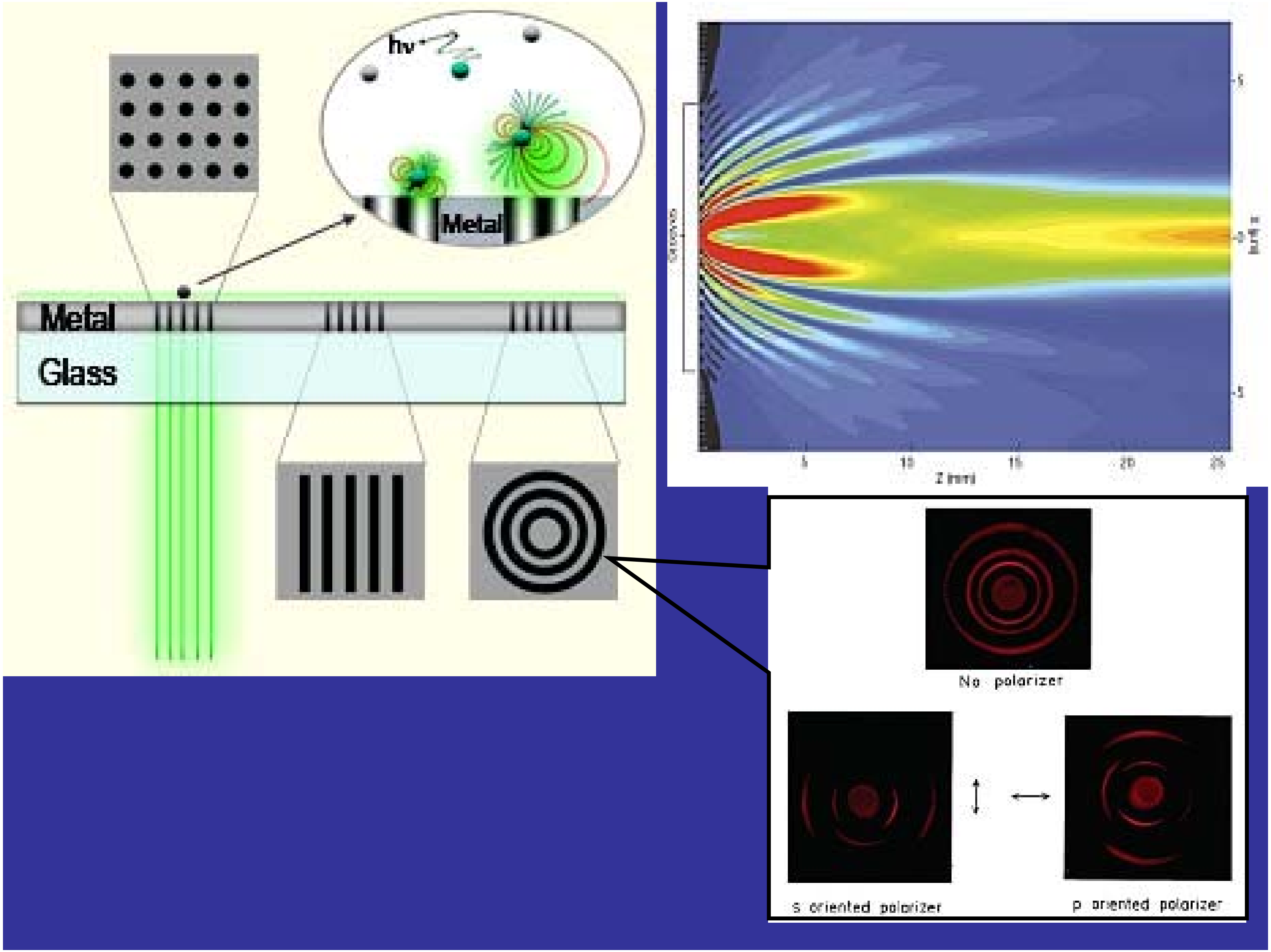
hν
Metal
Metal
Glass
5
10
15
20
25
Z (mm)
No polarizer
s oriented polarizer
p oriented polarizer

Overcoming the diffraction limit with the help of surface plasmons

metallic (Ag) film

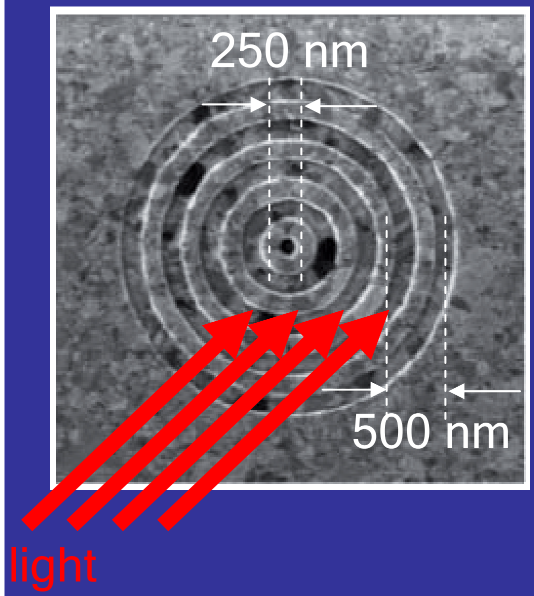

surface plasmon resonance @ 660nm

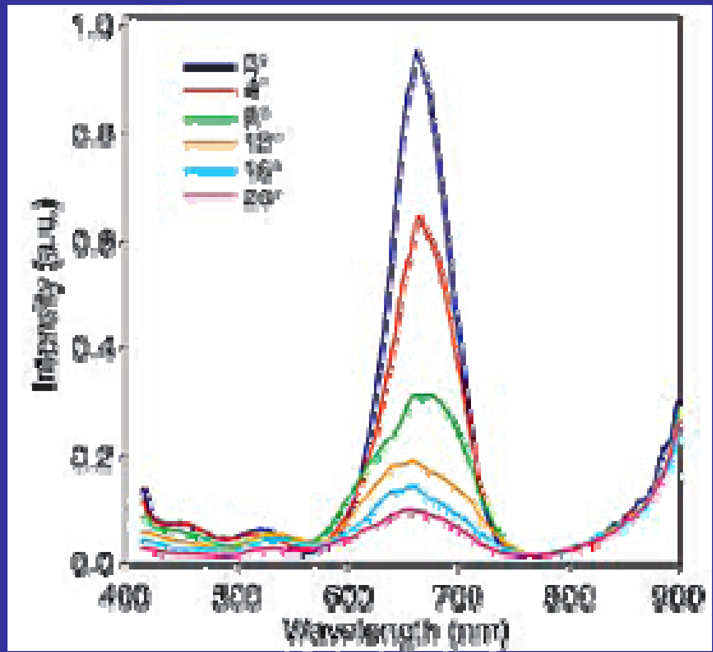

directionality is $\pm$ 3°

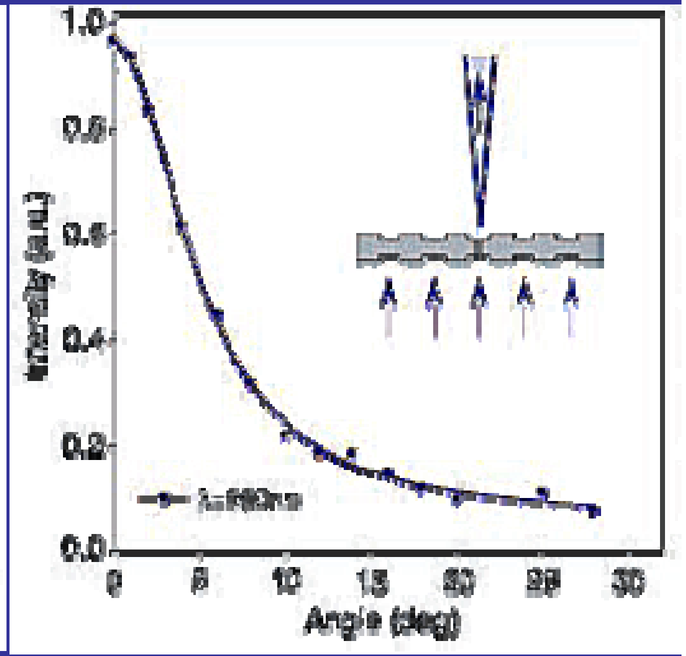

The coupling of light into SP modes is governed by geometrical momentum, selection rules (*i.e.*, occurs only at a specific angle for a given wavelength), the light exiting a single aperture will follow the reverse process in the presence of the periodic structure on the exit surface.

$$\underbrace{k_x\,(\text{outgoing})}_{k_{\text{plasmon}}} = \underbrace{k_x\,(\text{incoming})}_{nk\sin\theta} \pm \underbrace{NG}_{\text{reciprocal lattice vectors}}, \quad \text{where } G = 2\pi/d$$

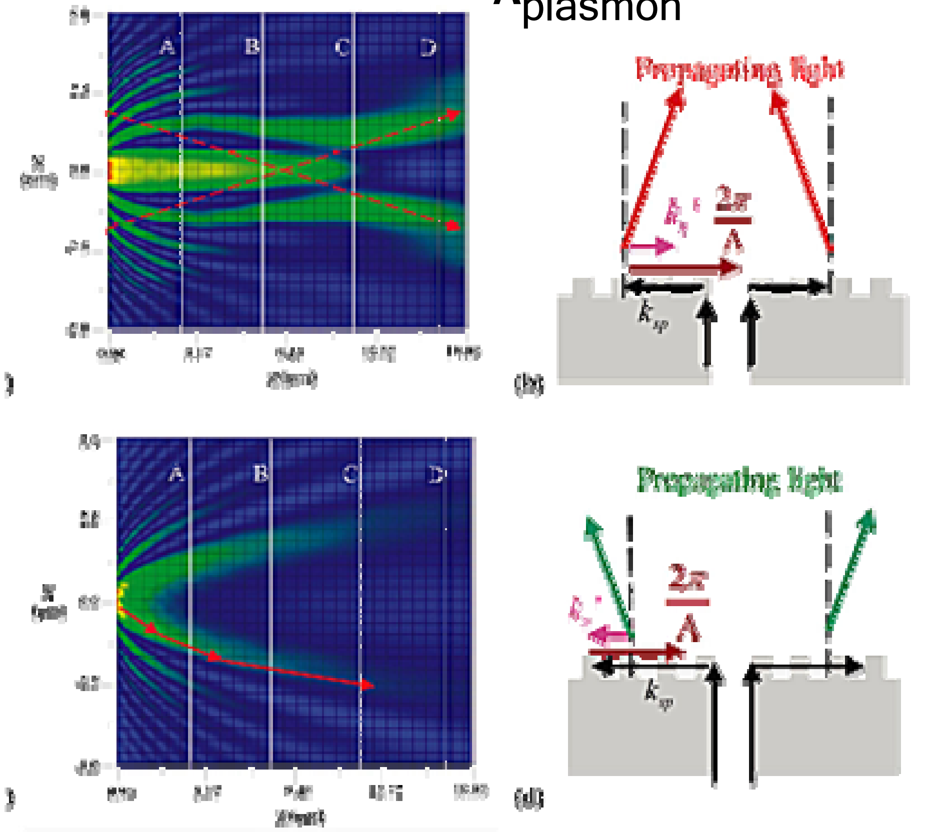

k_{SP}>G

k_{SP}<G

Yu et al., Phys. Rev. B 71, 041405 (2005)

Diffraction of nano-sized structures

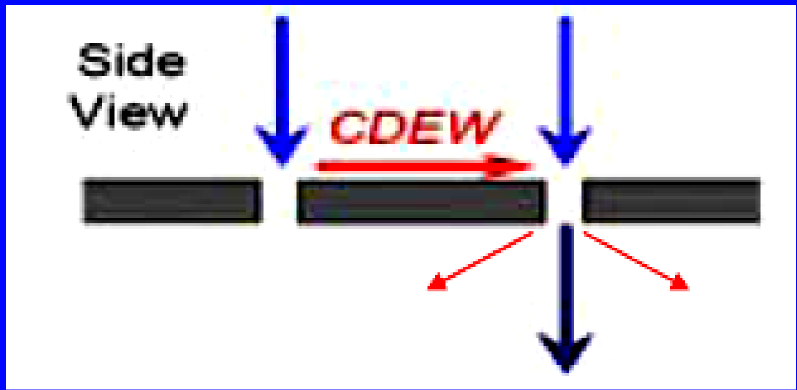

Lalanne et al. Nature Phy. (2006)
Gay et al. Nature Phy. (2006)

Constructive interference among the beams from slits;
Each slit is at F-P resonance
Interference of SW/SPP with incident wave

Remarks : Before arriving the slit, the two waves are of
Orthogonal polarizations
Orthogonal wave vectors ?
Their interference is done by mediation of SPP

How Conversion SPP/Light, and Interference occur ?

Field distribution *Ey*, *Hz*

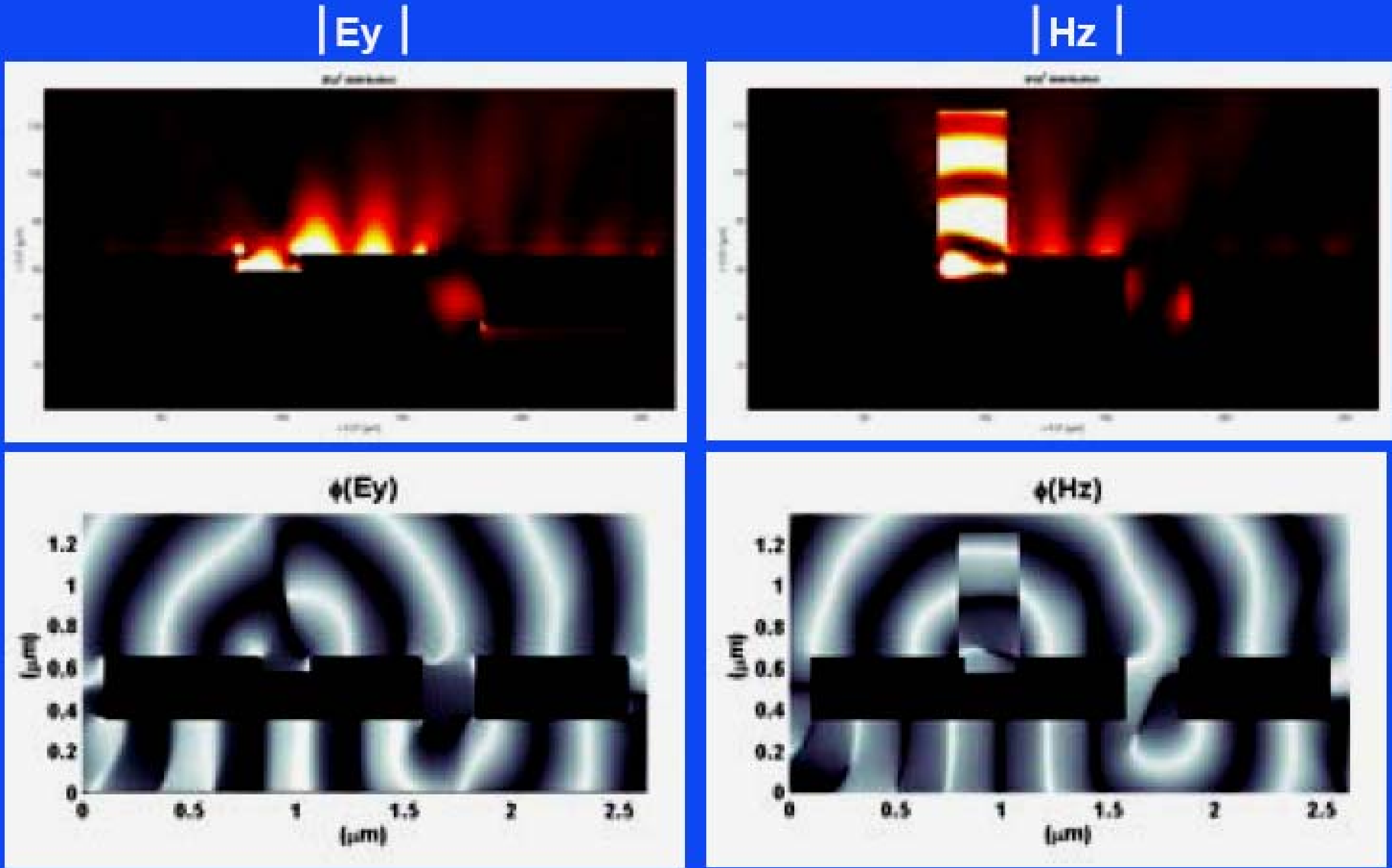

SPP coupling & Interference at nano-slit

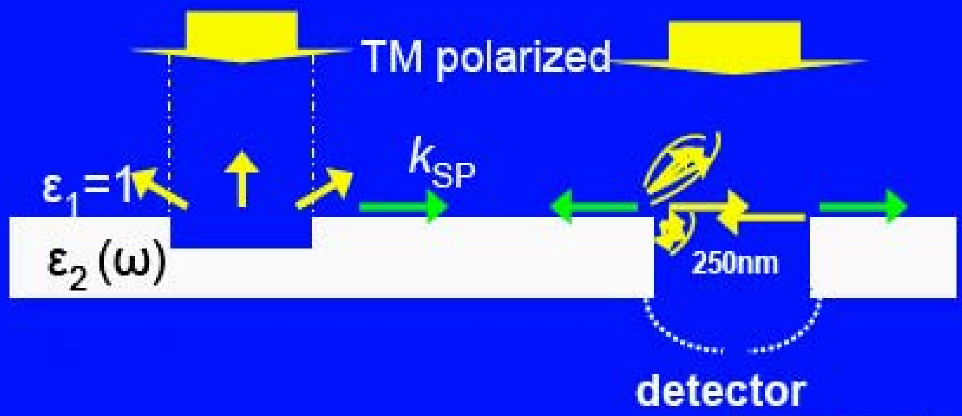

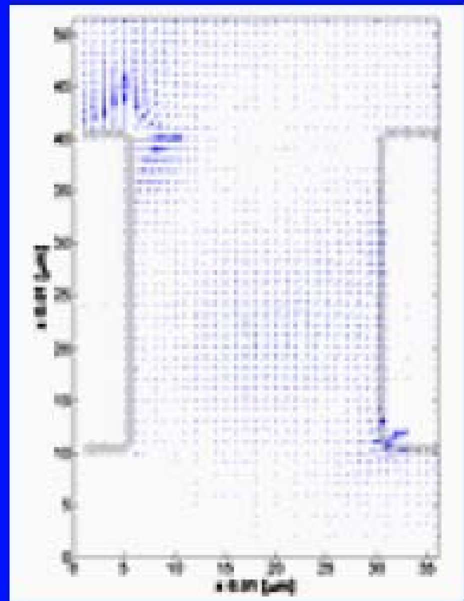

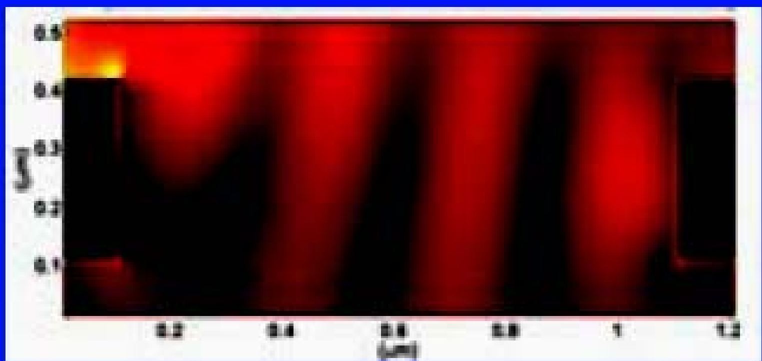

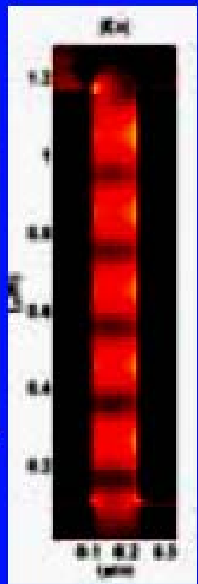

Coupling mechanism:
the incident SPP induces oblique dipole that reradiates Bulk waves and SPPs
Interference occurs at the slit.

Ung, Sheng, Opt. express (2007)
Invited Paper OSA Nanophotonic (2007)

F-P resonance of bulk H_z, E_y cross the slit

- When a>>λ, multiple reflections of bulk waves of Ey and Hz cross the slit as F-P resonance
- Oscillations of
  - Ey and Hz
  - Transmission
  - Scattered bulk wave
- Resonance mode in the slit normal to slit axis
- When a<λ, similar phenomenon

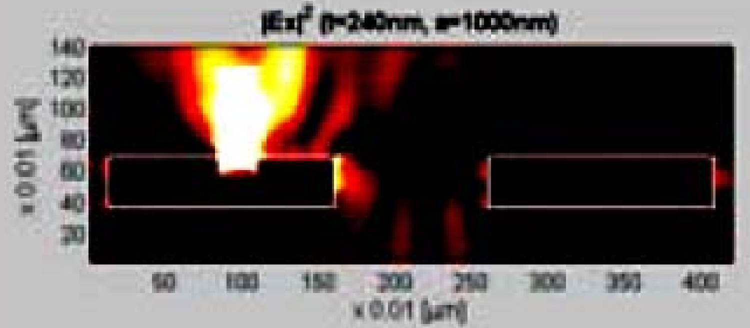

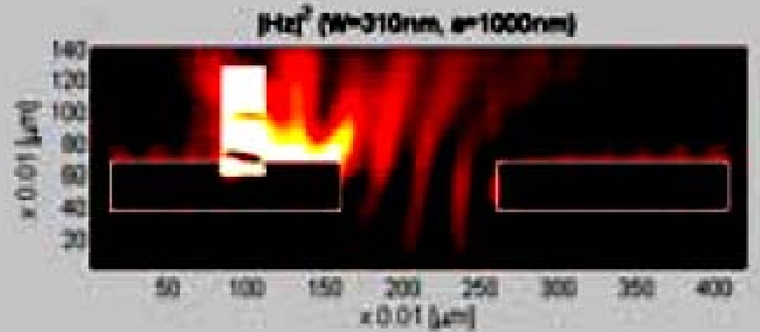

Demonstration of the Interference of SPP with incident beam (H_z field)

Constructive interference: *L* = 520nm

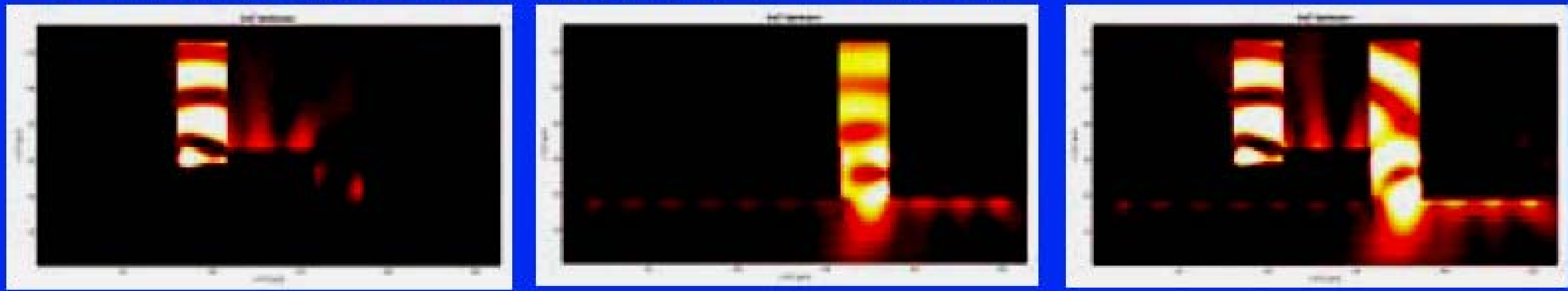

Destructive interference: *L* = 750nm

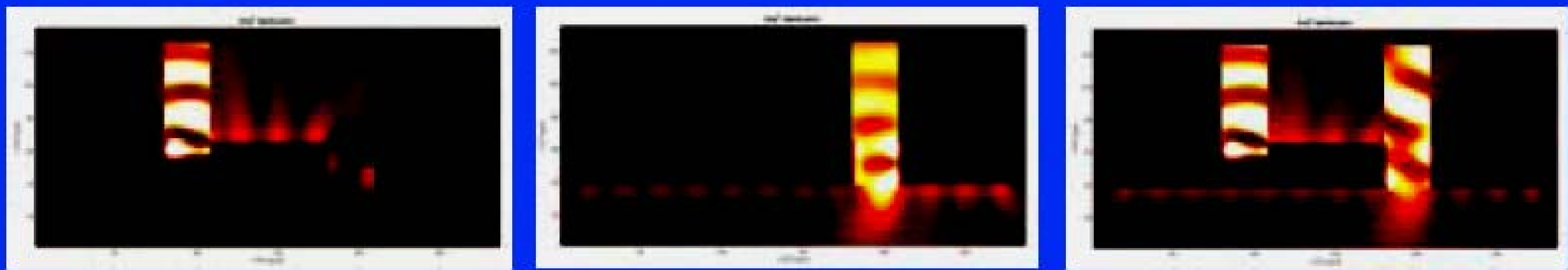

Slit width and thickness, *a* and *t*, are closed to optimal values

Induced dipoles in the slit

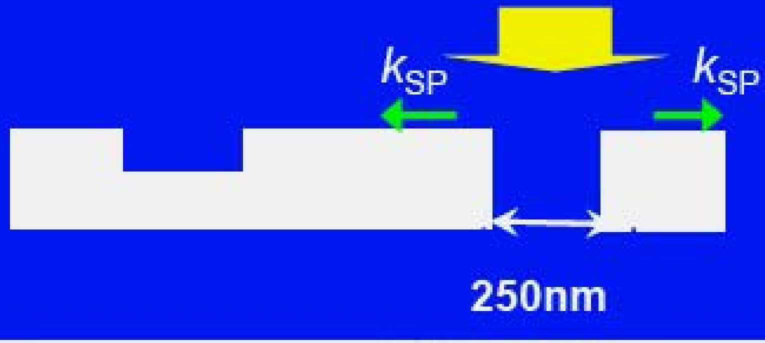

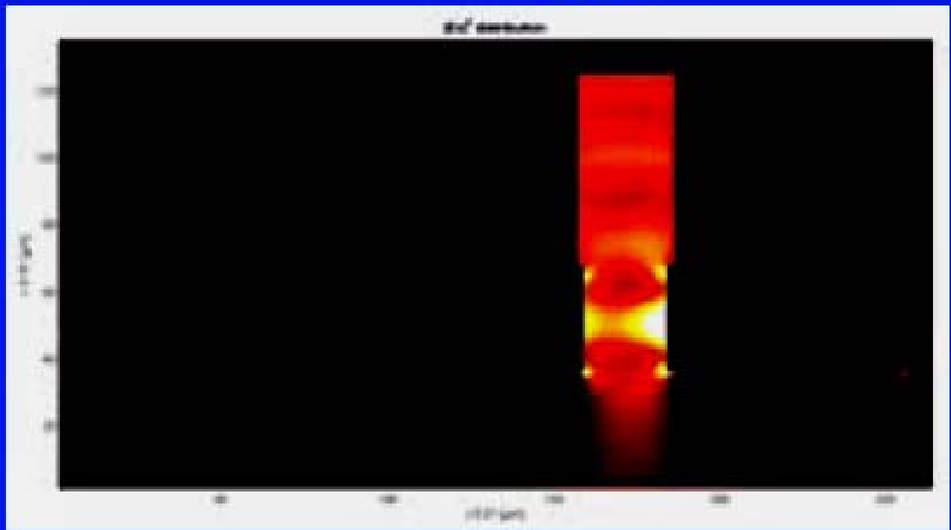

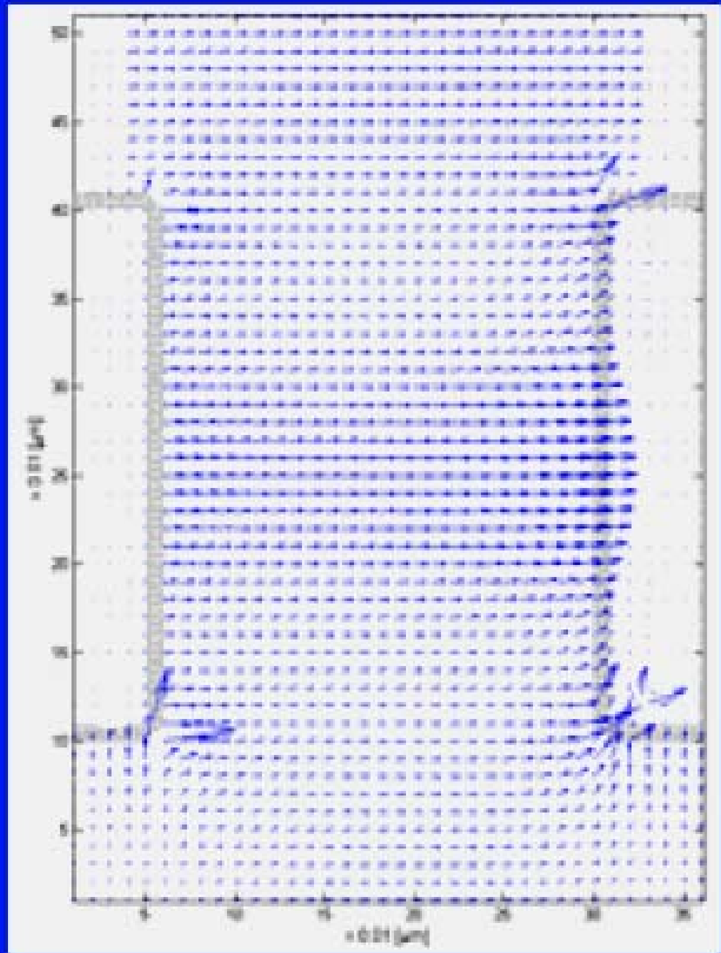

Two horizontal dipoles

Experiments of Gay Nature Physics 2006

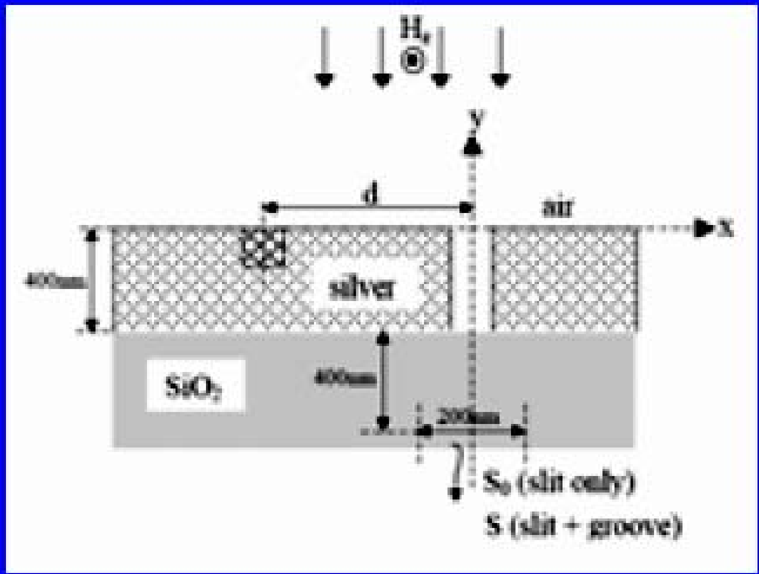

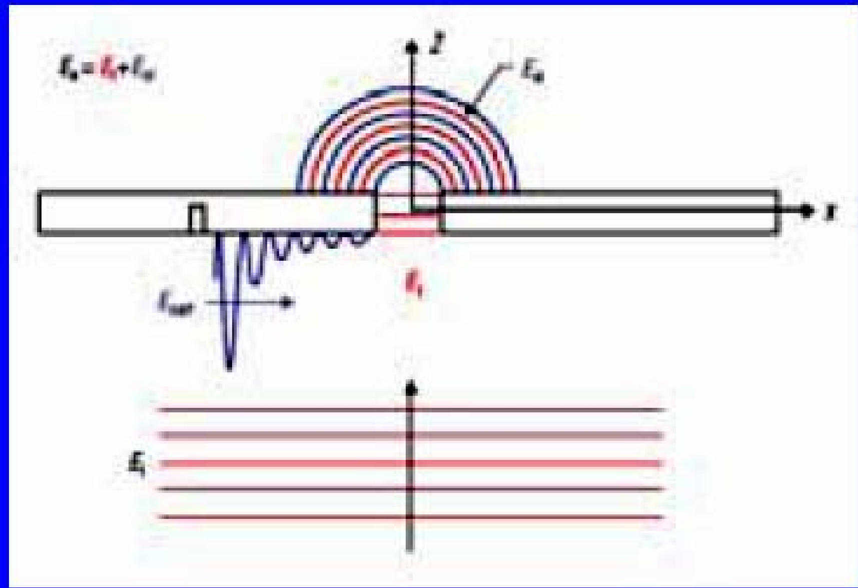

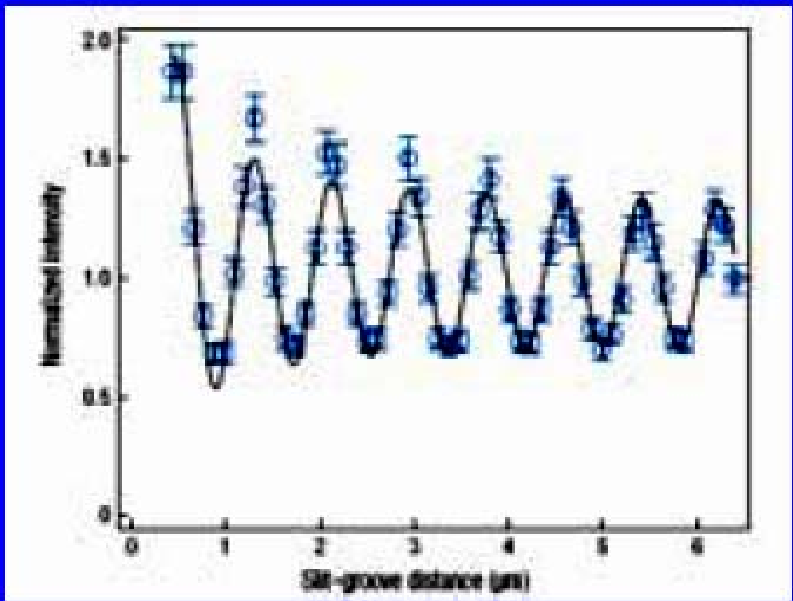

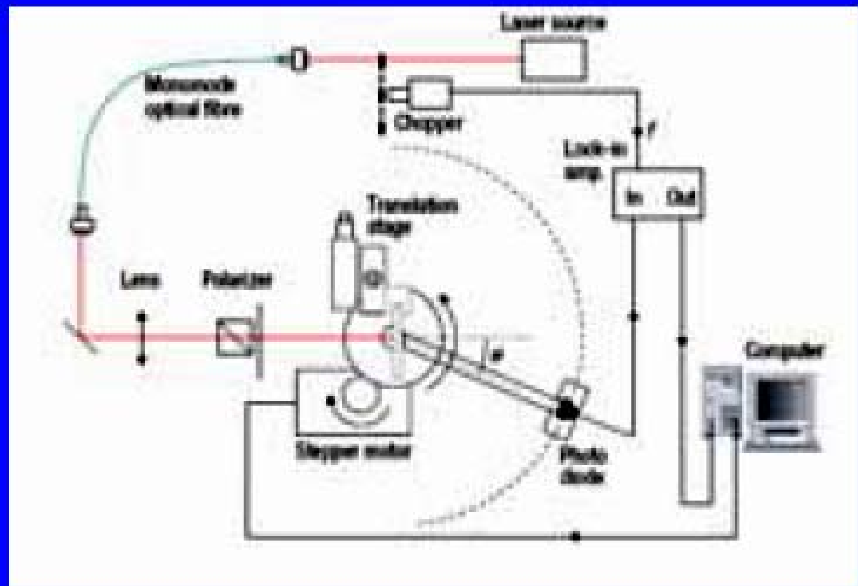

Creeping Waves Ph. Lalanne Nature Physics

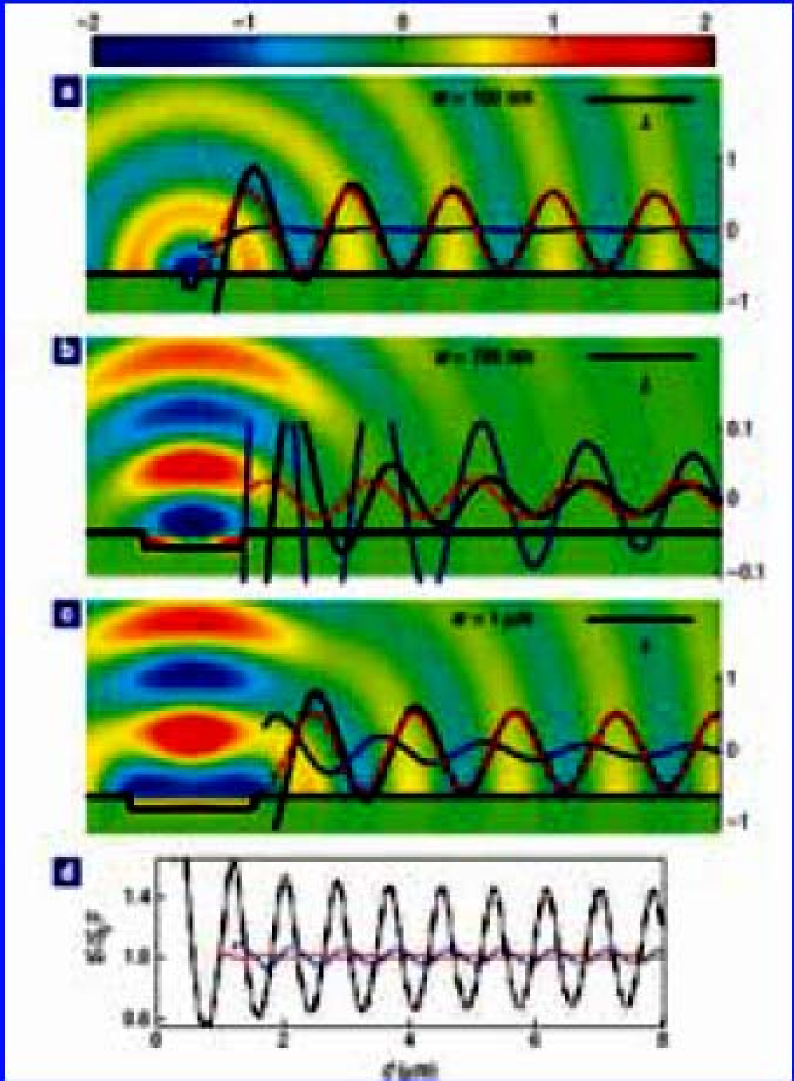

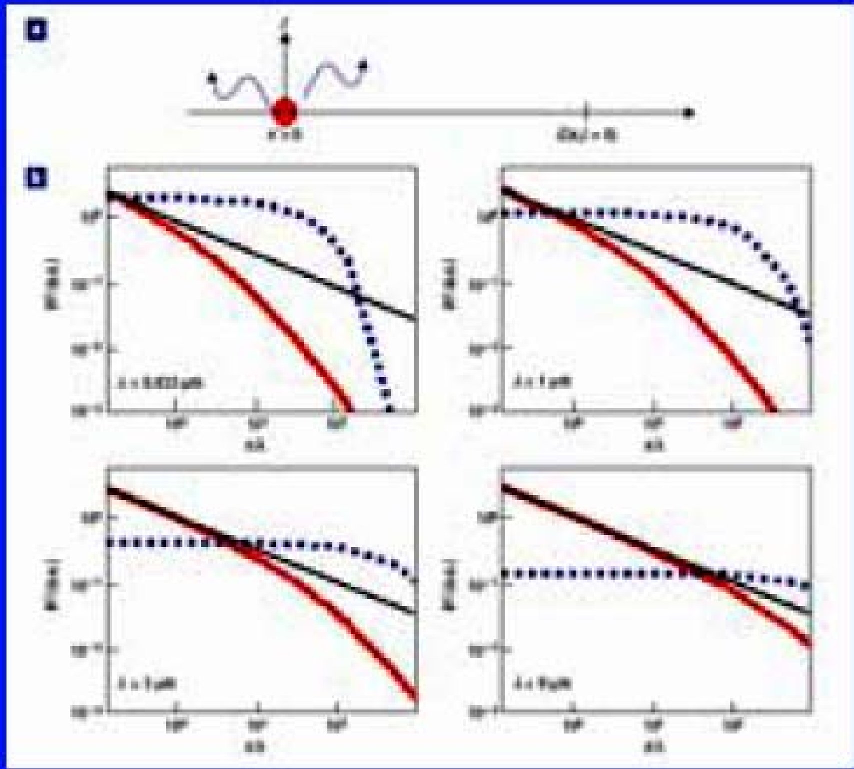

Sommerfeld Integral

$$I_m = \exp(-i\pi/4)\frac{\varepsilon_d}{\varepsilon_m-\varepsilon_d}\int_0^{\infty}\frac{\exp\left(ik_0x\sqrt{\varepsilon_m+it}\right)\sqrt{t}}{\left(1-(\varepsilon_m+it)k_0^2/k_{SP}^2\right)\sqrt{\varepsilon_m+it}}\,dt\ ;$$

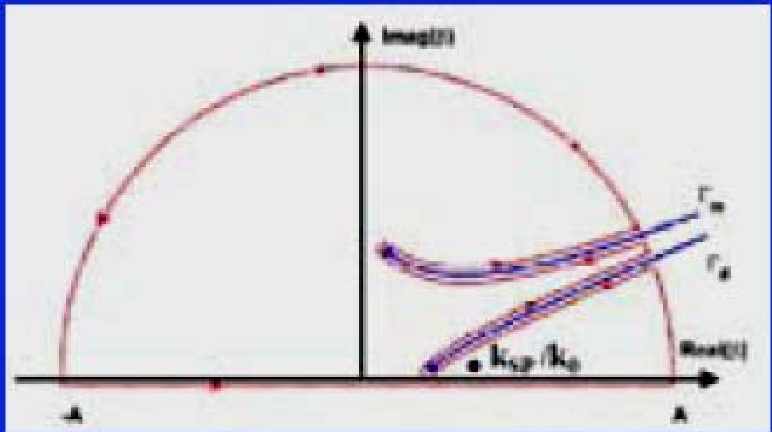

No exact closed-form solution is available
Difficult to evaluate numerically.

Transient behavior of surface plasmon polaritons scattered at a subwavelength groove

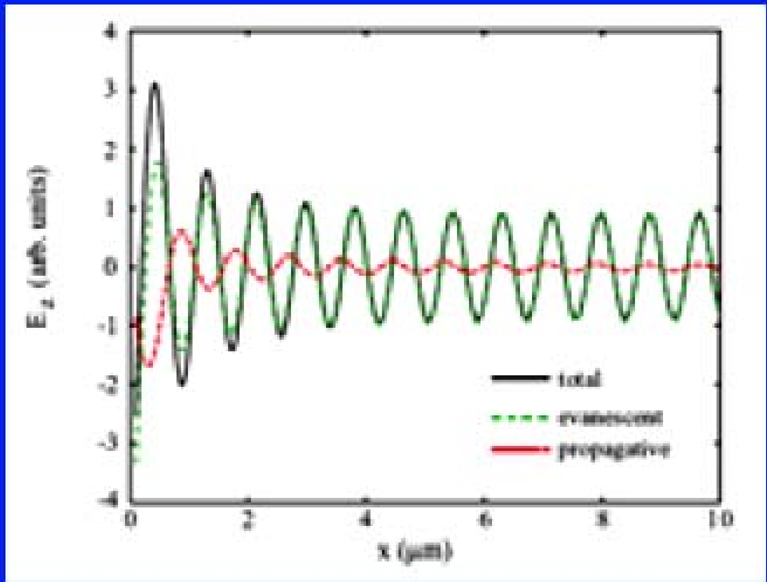

$$G(x) = i - \frac{\mathrm{Ei}(i(k_0 - q_{\mathrm{spp}})x)}{2\pi} + \frac{\mathrm{Ei}(i(-k_0 - q_{\mathrm{spp}})x)}{2\pi}.$$

Physics Rev B 2007

$$H_0(x) = i\omega J_m^* \left[\frac{(\varepsilon_d \varepsilon_m)^{3/2}}{\varepsilon_d^2 + \varepsilon_m^2} + \frac{1}{2\pi} \frac{k_{sp}^2}{k_0^2} E_1(-ik_{sp}x) \right] e^{ik_{sp}x}$$

Gravel, Sheng

Frequency-Dependent Materials in FDTD

$$\frac{H_{z(t;x,y+\Delta y,z\_}-H_{z(t;x,y-\Delta y,z)}}{2\Delta y}-\frac{H_{y(t;x,y,z+\Delta z)}-H_{y(t;x,y,z-\Delta z)}}{2\Delta z}=\tilde{\varepsilon}(x,y,z)\,\frac{E_{x(t+\Delta t;x,y,z)}-E_{x(t-\Delta t;x,y,z)}}{\Delta t}$$

$$\frac{H_{x(t;x,y,z+\Delta z)}-H_{x(t;x,y,z-\Delta z)}}{2\Delta z}-\frac{H_{z((t;x+\Delta x,y,z)}-H_{z(t;x-\Delta x,y,z)}}{2\Delta x}=\tilde{\varepsilon}(x,y,z)\,\frac{E_{y(t+\Delta t;x,y,z)}-E_{y(t-\Delta t;x,y,z)}}{\Delta t}$$

$$\frac{H_{y(t;x+\Delta x,y,z)}-H_{y(t;x-\Delta x,y,z)}}{2\Delta x}-\frac{H_{x(t;x,y+\Delta y,z)}-H_{x(t;x,y-\Delta y,z)}}{2\Delta y}=\tilde{\varepsilon}(x,y,z)\,\frac{E_{z(t\_\Delta t;x,y,z)}-E_{z(t-\Delta t;x,y,z)}}{\Delta t}$$

where $\mathbf{E}=E(E_x,E_y,E_z)$ and $\mathbf{H}=H(H_x,H_y,H_z)$ are the electric field and the magnetic induction vectors, respectively, and 2Δx, 2Δy, 2Δz are increments along the three coordinate directions respectively, Δt is the unit time increment, and (x,y,z) is the complex dielectric constant of the medium at that point.

Equations are simultaneously solved to determine the component values at the time $t+\Delta t$.

FDTD—Finite-Difference Time-Domain method

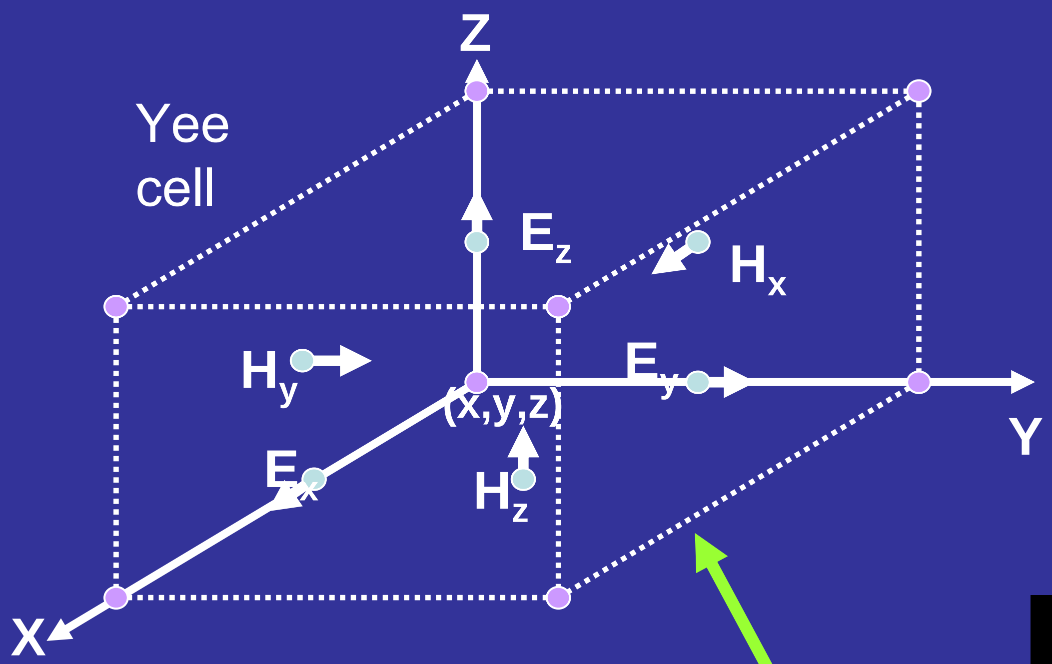

Spatially stagger the vector components of the E-field and H-field :
spatial accuracy 2nd order (Yee) or higher

⇨ E and H are discrete in space

Yee cell

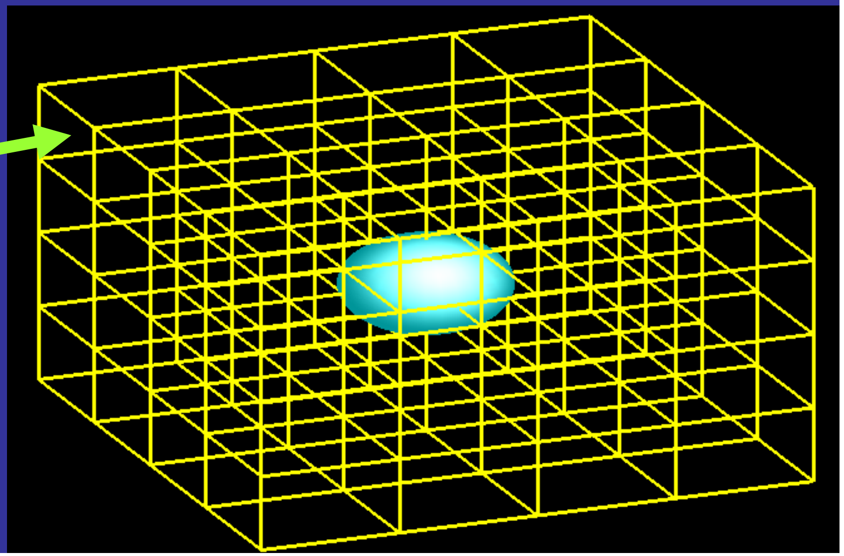

$$\Delta t \le 1/c\sqrt{\Delta x^{-2} + \Delta y^{-2} + \Delta z^{-2}}$$

Many challenges when implementing it to cover wide applications

Kane Yee (1966). "Numerical solution of initial boundary value problems involving Maxwell's equations in isotropic media". *Antennas and Propagation, IEEE Transactions on* **14**: 302–307.

FDTD—Finite-Difference Time-Domain method

Solving Maxwell's equations directly : full vectorial method

$$\frac{\partial B}{\partial t} = -\nabla \times E \qquad \frac{\partial D}{\partial t} = \nabla \times H \qquad \nabla \bullet D = \rho \quad \nabla \bullet B = 0 \qquad D = \varepsilon E \quad B = \mu H$$

E and H are discrete in time $\vec{E}(t) \rightarrow \vec{E}^{\,n\Delta t} \qquad \vec{H}(t) \rightarrow \vec{H}^{\,(n+\frac{1}{2})\Delta t}$

The basic FDTD time-stepping relation:

$$\vec{E}^{\,n+1} = \vec{E}^{\,n} + \alpha \vec{\nabla} \times \vec{H}^{\,n+1/2}$$

$$\vec{H}^{\,n+3/2} = \vec{H}^{\,n+1/2} + \beta \vec{\nabla} \times \vec{E}^{\,n+1}$$

Leap-Frog Scheme

$$\vec{E}^{\,0} \longrightarrow \vec{H}^{\,1/2} \longrightarrow \vec{E}^{\,1} \longrightarrow \vec{H}^{\,3/2} \longrightarrow \cdots$$

2nd order accurate in time: error ~ Δt^2

What are Dispersive Materials?

- Dispersive materials
  - have electrical parameters (permittivity and conductivity) which vary significantly as a function of frequency
- Examples include water, metals, body tissue, plasmas and more
- Many typical materials are frequency-independent and the dispersive models are not needed

When to use Dispersive Material Capabilities in FDTD?

- Broad-band output is desired from a geometry containing this type of material

- In any simulation (broad-band or single frequency) in which the electrical parameters for the material would cause the calculation to become unstable (for example negative permittivities)

Types of Dispersive Models in FDTD

- Debye
  - useful for materials with condensed polar molecules such as water
- Drude
  - similar to the Debye model
  - with an added electrical conductivity term
  - Also available for magnetic materials
- Lorentz
  - used to describe absorption bands
  - often in the optical frequency range
- Magnetized Ferrites
  - Discussed in a separate section of these notes

Dispersive Technique in FDTD

- ✓ FDTD uses an improved implementation of the Recursive Convolution Technique for dispersive materials

- ✓ Separate Total Field and Scattered Field formulations for increased accuracy when incident plane wave excitation is specified

- ✓ Increases memory load and execution time moderately

- ✓ Second order accuracy

The Debye Model

- Describes the time-domain exponential decay in the permittivity
  - due to the alignment of dipolar molecules to an applied field
- Typical example is water
  - many materials with high water content have similar characteristics

The Debye Model Parameters

- The Debye permittivity is described by the equation

$$\varepsilon(\omega) = \varepsilon_\infty + \frac{\varepsilon_s - \varepsilon_\infty}{1 + j\omega\tau_0}$$

Limits on Debye Parameters

- In order to produce a realistic material and a stable calculation, some limits are placed on the parameters

- The imaginary part of the complex permittivity may not be negative

- Infinite frequency permittivity $\geqslant$ 1

- Static permittivity > infinite frequency permittivity

Complex Permittivity for Water

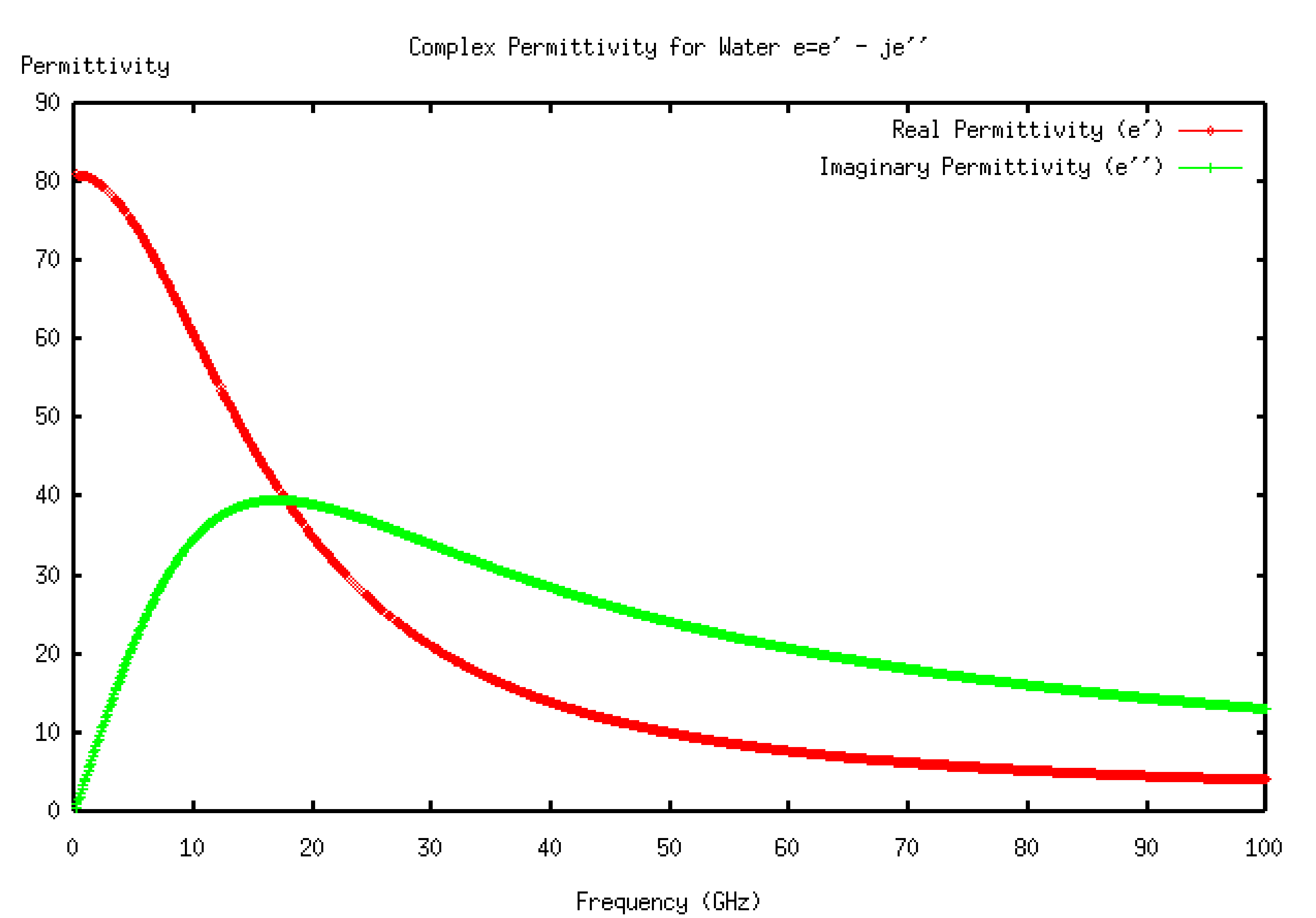

Permittivity and Conductivity for Water

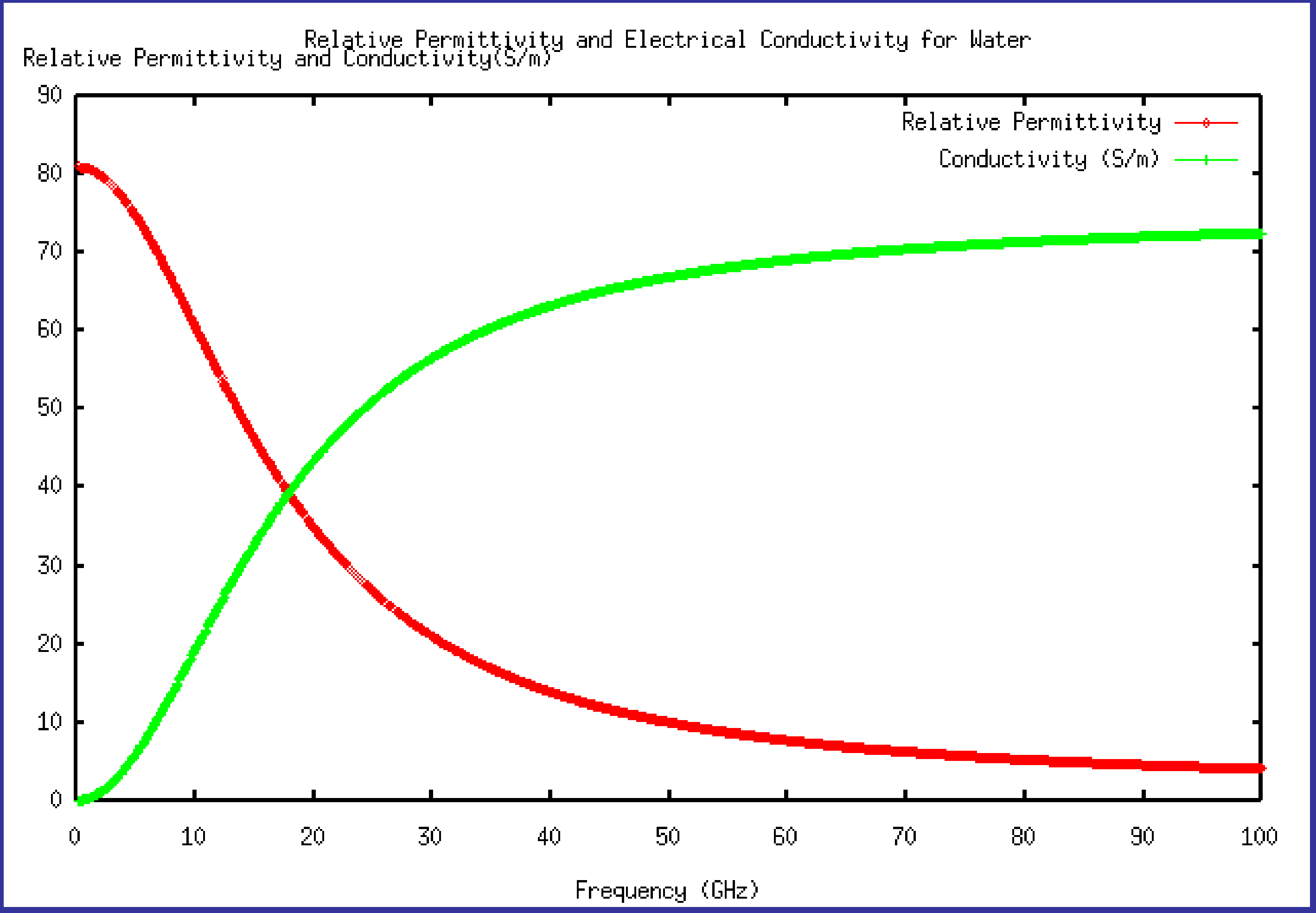

Effect of Debye Parameters

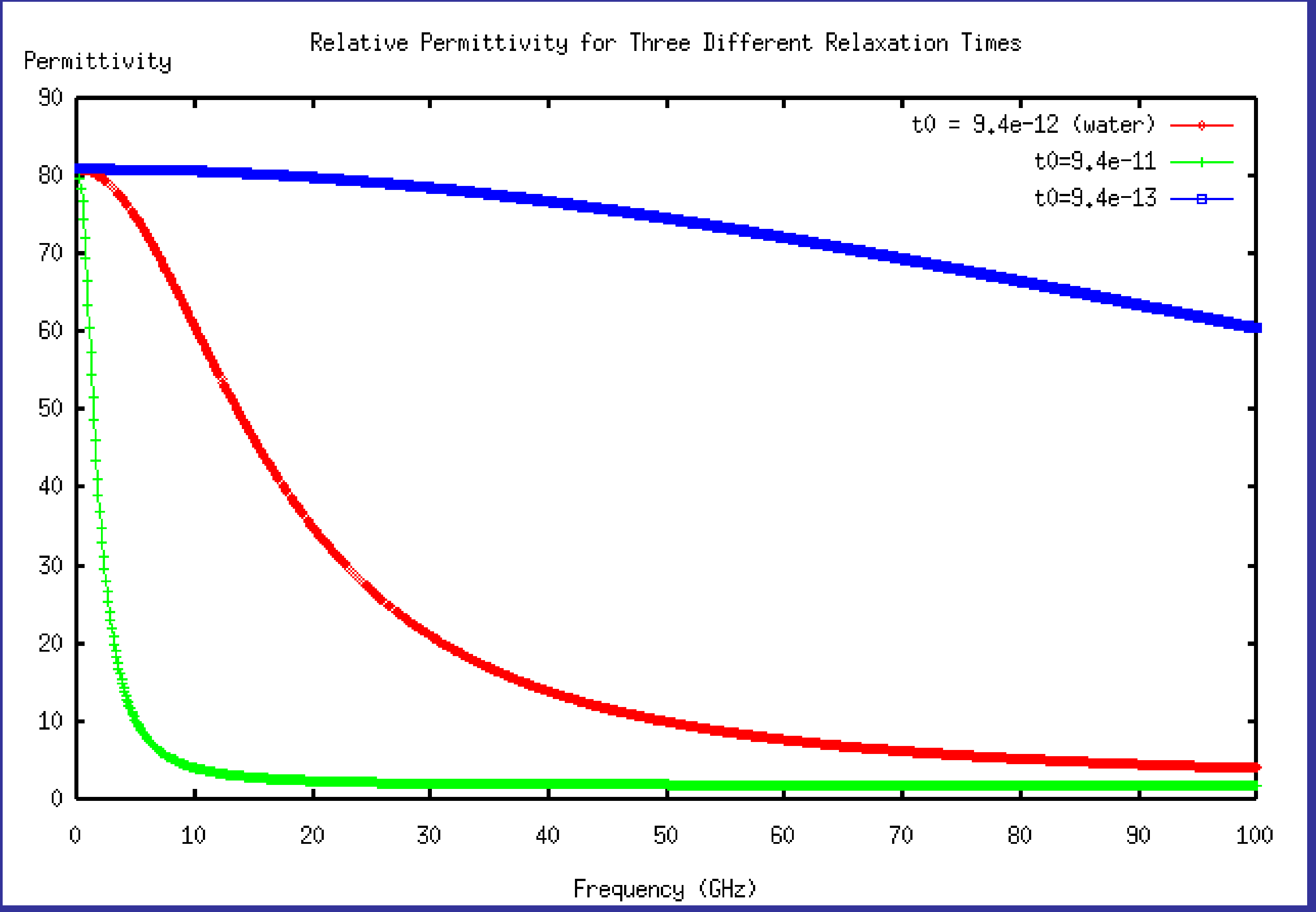

The Drude Model

- The Drude model describes a material similar to the Debye model
  - with the addition of an electrical conductivity term
  - where σ is the conductivity.

$$\varepsilon(\omega) = \varepsilon_\infty + \frac{\varepsilon_s - \varepsilon_\infty}{1 + j\omega\tau_0} + \frac{\sigma}{j\omega\varepsilon_0}$$

Simple Drude Model Limits

- Simplified limits for Drude model:
  - identical to those of Debye ($\varepsilon_\infty \geqslant 1$, $\varepsilon_s > \varepsilon_\infty$)
  - with added condition that electrical conductivity (σ) < 0
- Limited set of materials fit this condition
- More general conditions available

General Drude Model Limits

- Infinite Frequency Permittivity (ε_∞) ≥ 1
- If $\varepsilon_s > \varepsilon_\infty$ then $\sigma \geq 0$
- If $\varepsilon_s < \varepsilon_\infty$, then the conductivity must satisfy the condition

$$\sigma \geq \frac{\varepsilon_0(\varepsilon_\infty - \varepsilon_s)}{\tau_0}$$

Example Drude Materials

- Isotropic Plasmas
- Metals such as gold, aluminum, and chromium at optical frequencies
- Some biological tissues
- Negative Index Materials (NIM), Double Negative (DNG) materials

Techniques for Using Drude

- Some materials, such as plasmas, fit the Drude model exactly
- For the general case
  - a curve-fitting technique should be used to find the best-fit parameters for the Drude model
- Curve-fitting used for following metal examples

Complex Perm for Drude Plasma

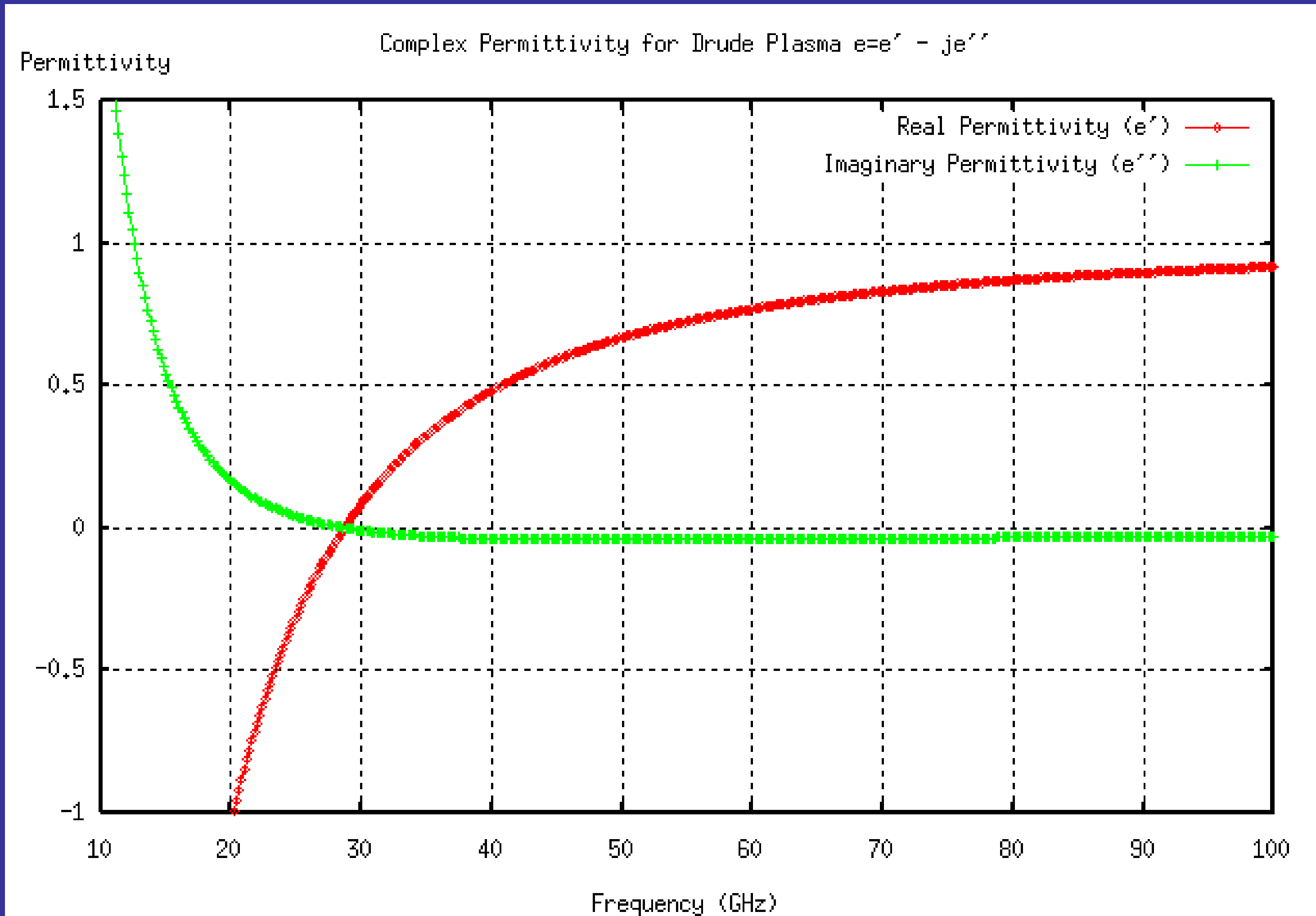

Complex Permittivity For Gold

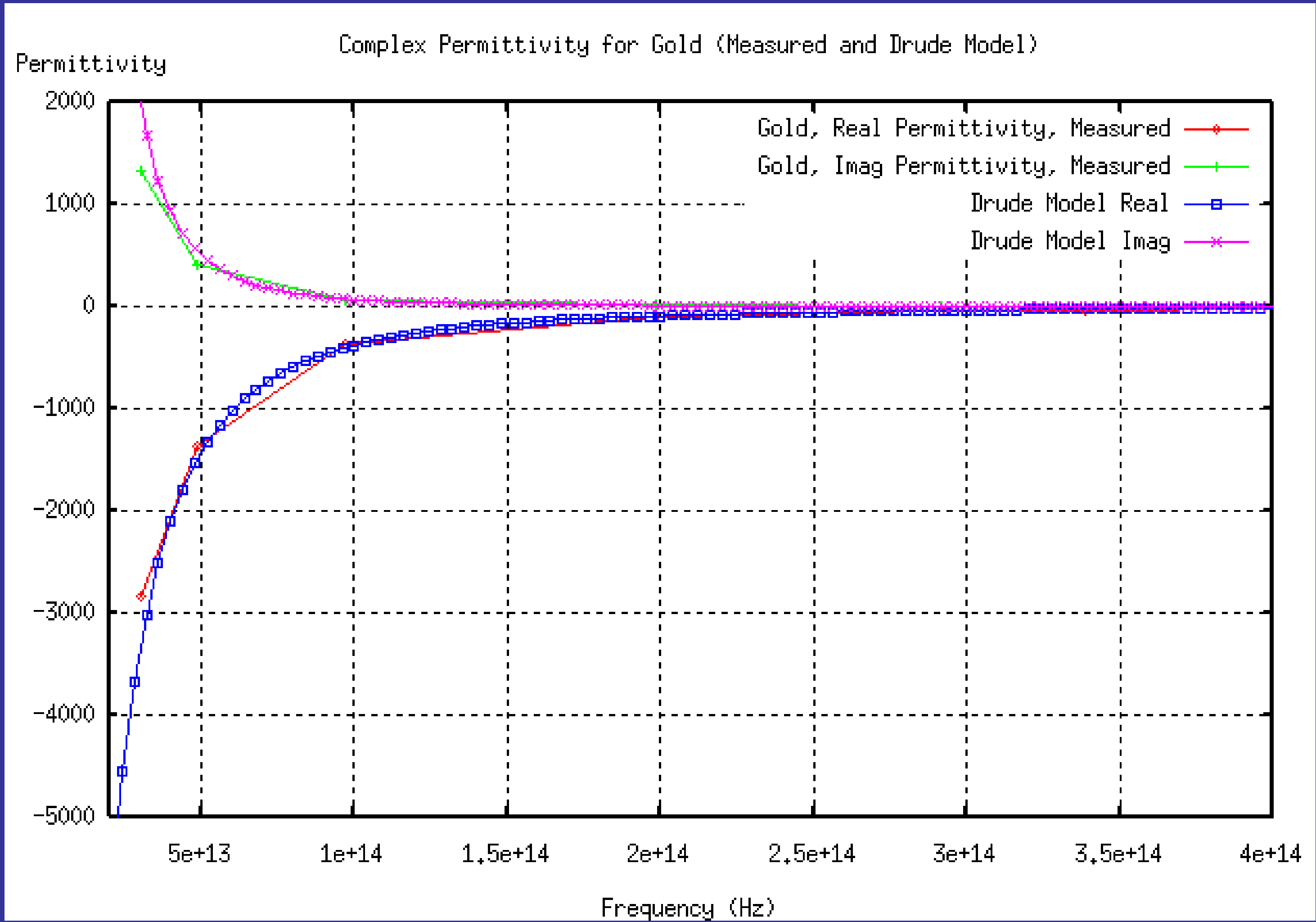

The Lorentz Model

- Characterized by a high resonance in the permittivity at a single frequency
- Infinite and static permittivity values as with Debye
- Resonant frequency and damping coefficient values define the peak permittivity

The Lorentz Model Expression

The Lorentz complex permittivity is defined as

$$\varepsilon(\omega) = \varepsilon_\infty + (\varepsilon_s - \varepsilon_\infty)\frac{\omega_0^2}{\omega_0^2 + 2j\omega\delta - \omega^2}$$

where ω_0 is the resonant frequency and δ is the damping coefficient, both in radians/second

Limits on the Lorentz Parameters

- As with Debye, $\varepsilon_s > \varepsilon_\infty$
- $\omega_0 > 0$ and $\delta > 0$
- A conductivity value (σ) may also be used and it must be ≥ 0

Example Lorentz Complex Permittivity

- $\varepsilon_s = 2.25$, $\quad = 1.0$
- $\omega_0 = 4.0 \times 10^{16}$, $\delta = 0.28 \times 10^{16}$
- $\sigma = 0$

Complex Perm for Lorentz

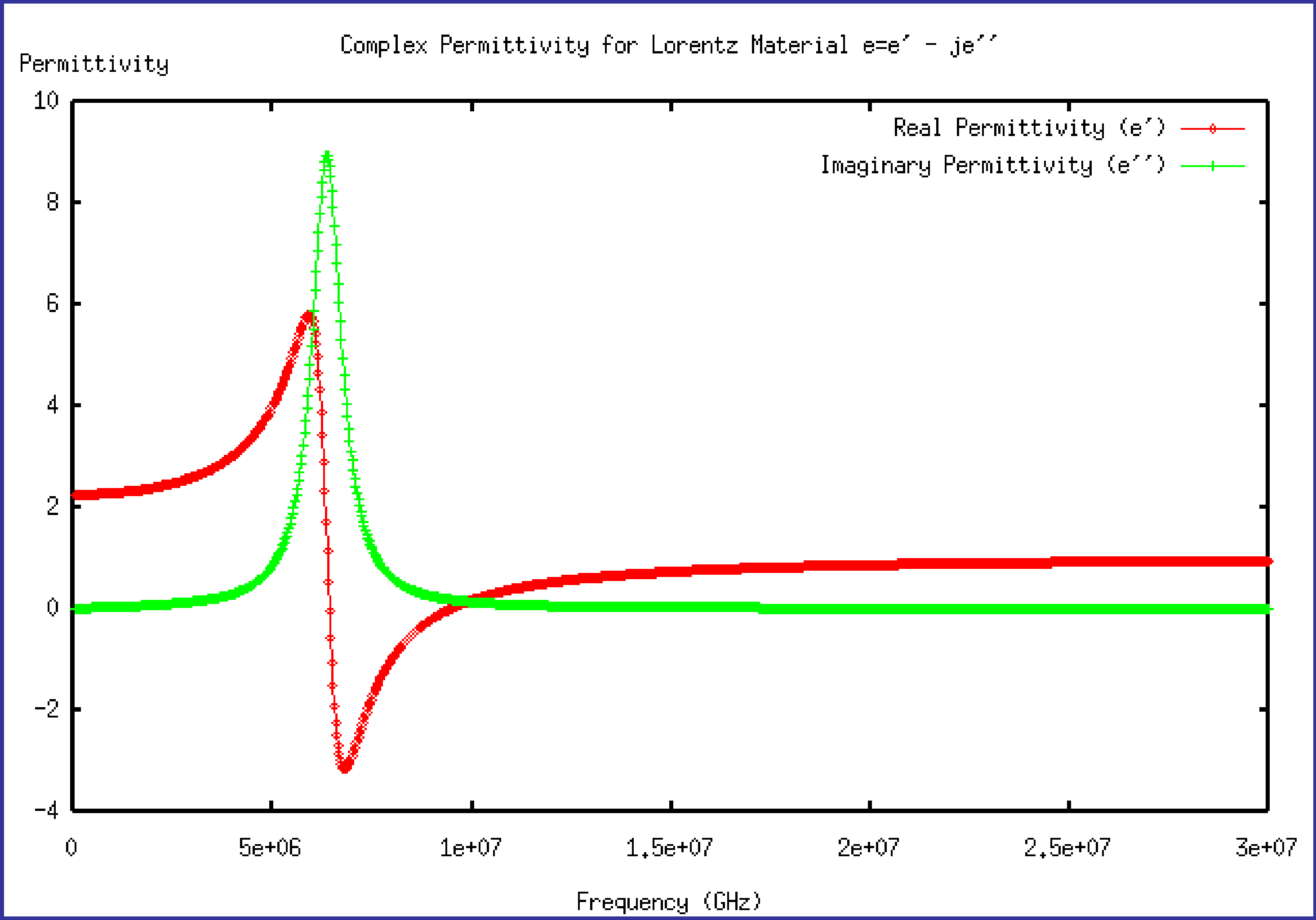

XFDTD Electrical Material Parameters

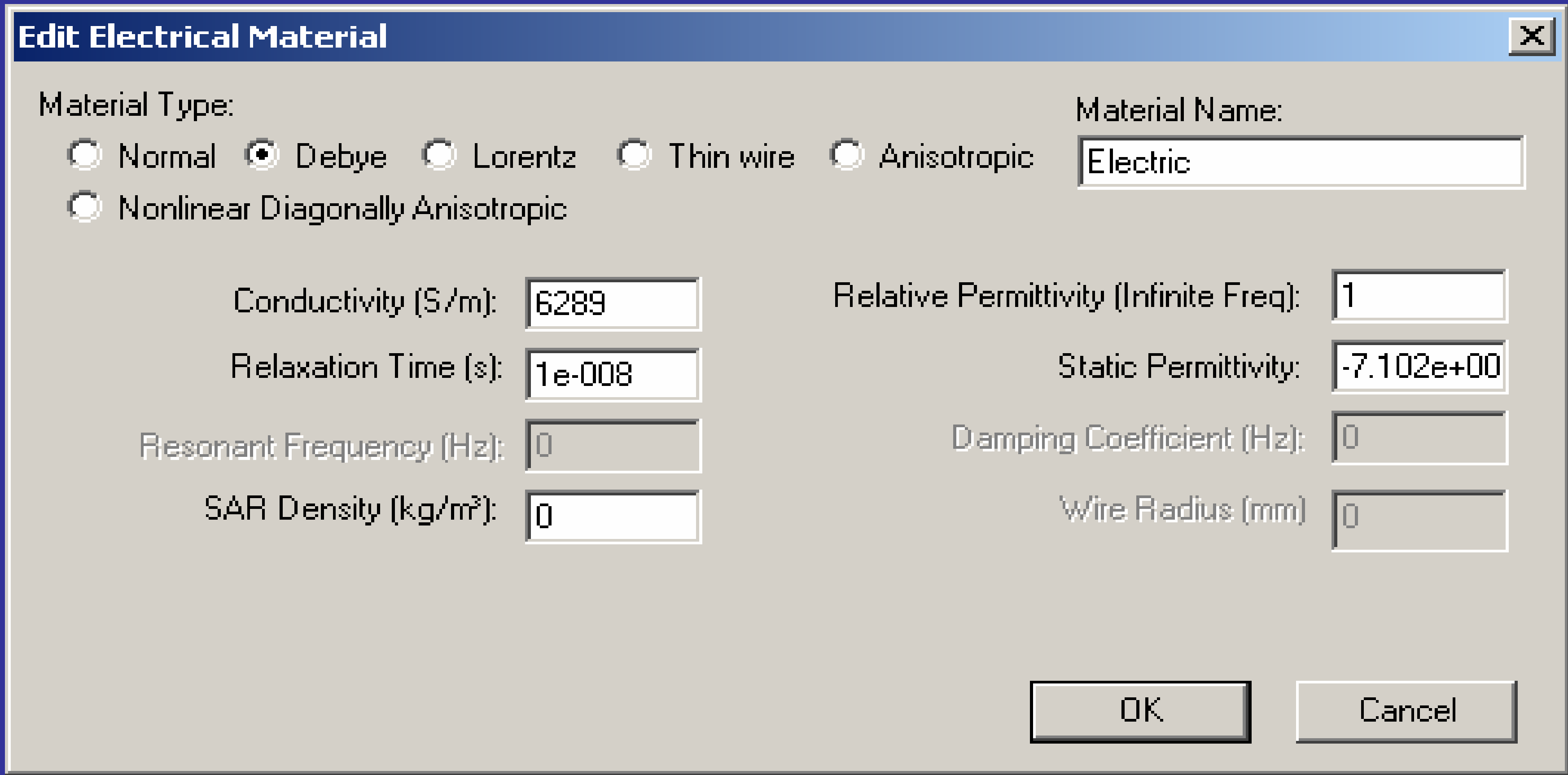

Dispersive XFDTD Examples

- Examples are for radar cross-section (RCS) results versus frequency for a sphere

- An analytical solution (Mie Series) is readily available for this case for validation

- Drude materials are used as they are the most commonly encountered

Drude Plasma Example

- A 3.75 mm radius plasma sphere is simulated using the Drude model.
- Broad-band RCS at a single angle computed
- Both staircased and dielectric-conformal meshing (coming in XFDTD 6.3) spheres simulated
- This example comes directly from
  "FDTD Calculation of Scattering From Frequency-Dependent Materials" by Raymond Luebbers, David Steich, and Karl Kunz, IEEE Transaction on Antennas and Propagation, Vol. 41, No. 9, September 1993.

Drude Plasma Example (2)

- Cell size of 150μm is used (25 FDTD cell radius for sphere)
- XFDTD Parameters: τ_0=5 x 10^{-11}, σ=14.396, ε_∞=1, ε_s=-80.295
- 71x71x71 cell space with 10 cell borders
- 10 cells/wavelength at maximum frequency
- Gaussian Pulse plane wave with width of 32 time steps is incident

RCS of Drude Plasma Sphere

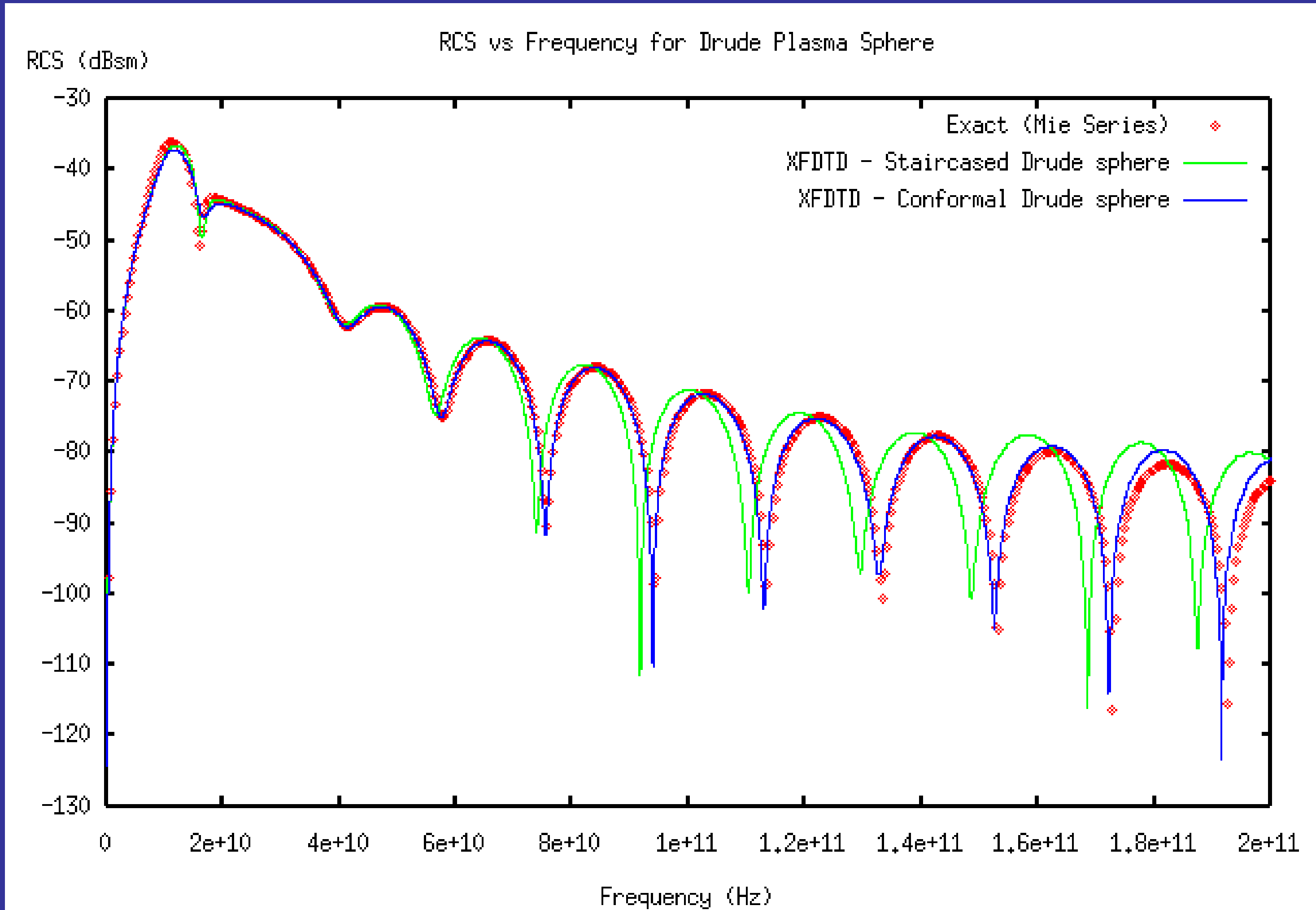

Optical Frequency Gold Sphere

- At optical frequencies many metals exhibit Drude characteristics
- A material of high current interest is gold
- RCS is computed for a 75nm radius sphere
- A curve-fit Drude model is used for Gold with parameters ε_∞= 9.012, ε_s=-12990, σ=1.276 x 10^7, τ_0=9.02 x 10^{-15}

Gold Sphere XFDTD Calculation

- A Gaussian pulse plane wave is incident with width 32 time steps
- 25,000 time steps are run in a 71x71x71 cell space
- Sphere radius is 25 cells with 3nm cell size
- Both staircased and dielectric-conformal spheres simulated

RCS of Drude Plasma Sphere

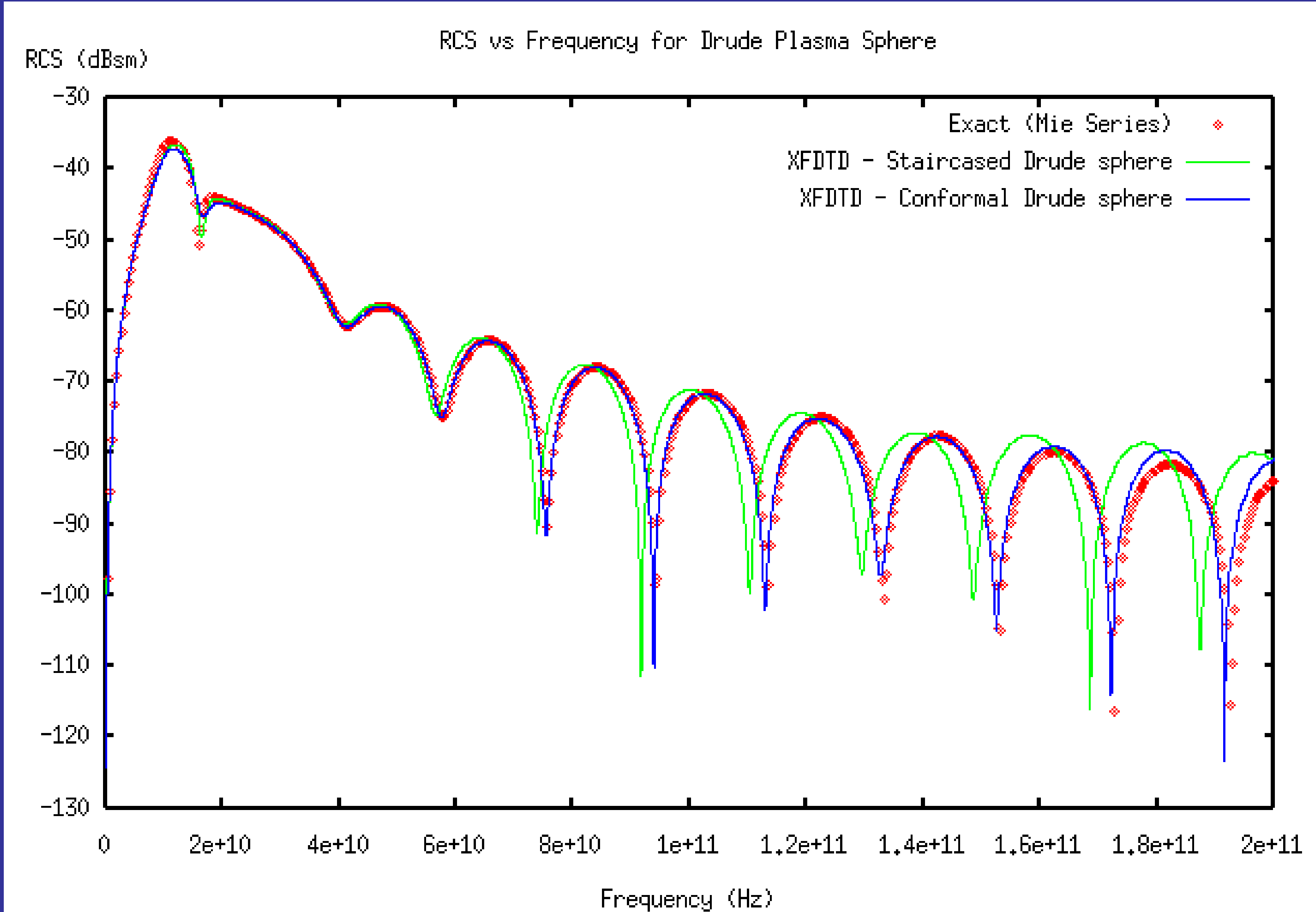

Ez Field in XZ Plane with Hollow DNG Sphere at 20 GHz

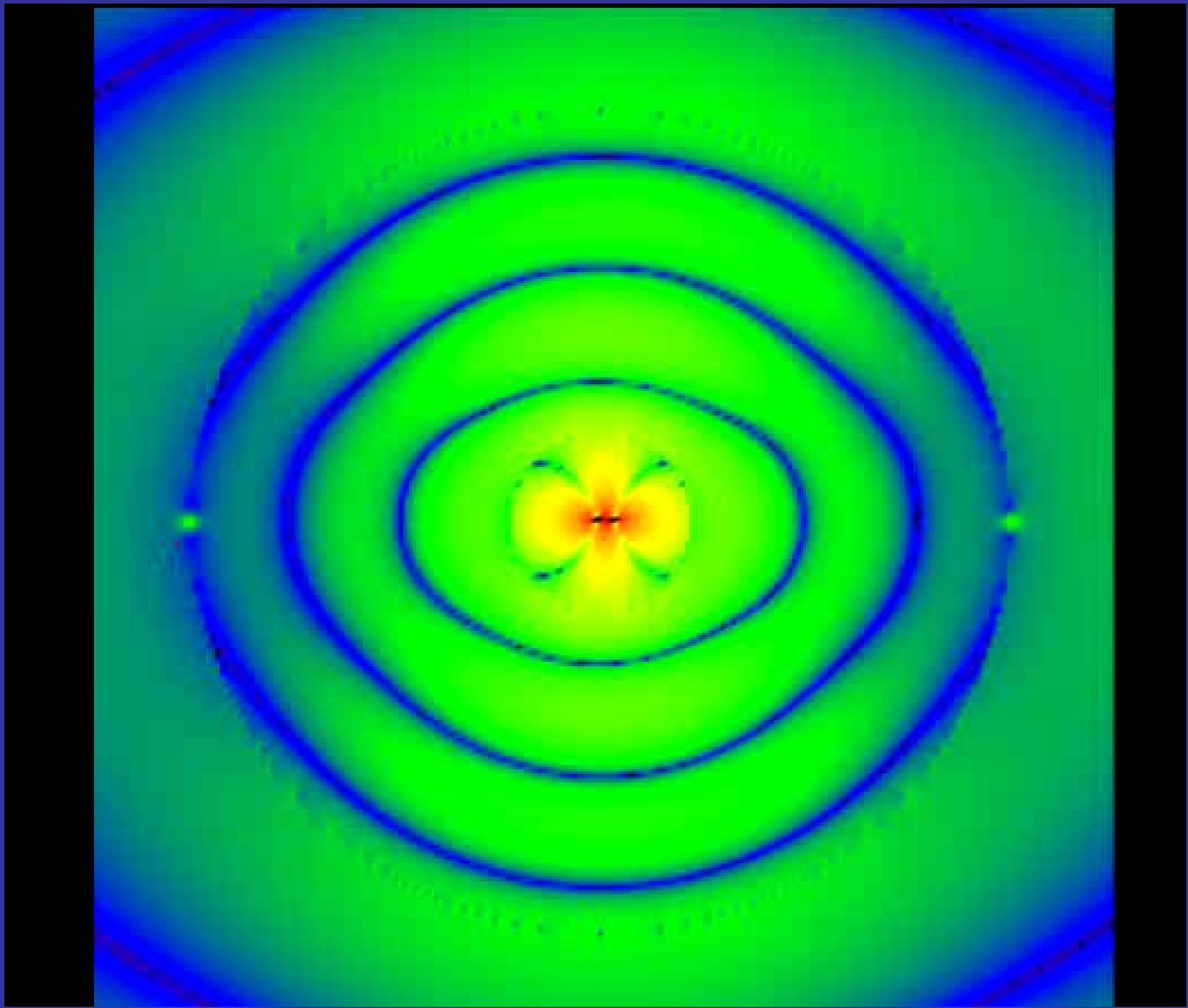

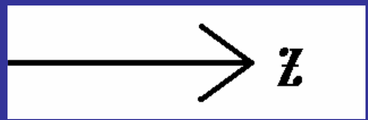

Discrete dipole approximation

Electrodynamic Analysis of Localized Surface Plasmon

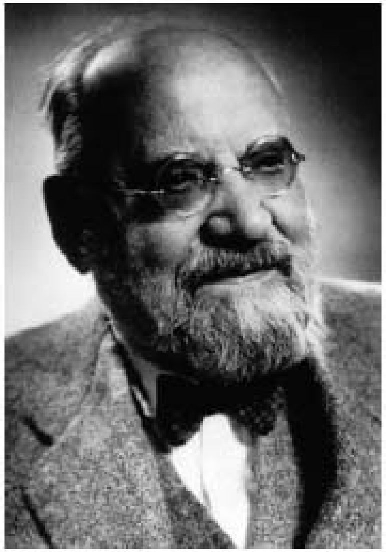

Gustav Mie

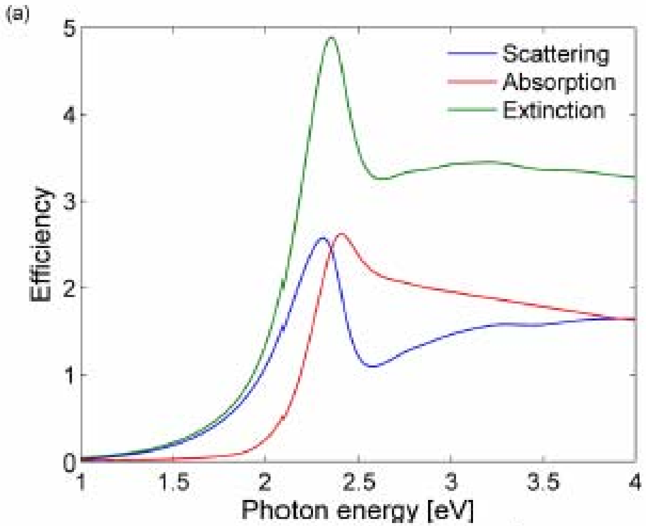

60-nm Au nanosphere in free space

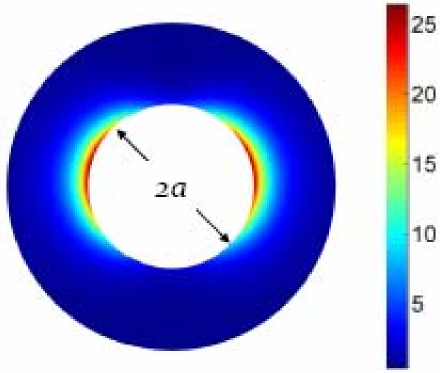

Near field enhancement

Discrete Dipole Approximation
Finite Different Time Domain
T-matrix

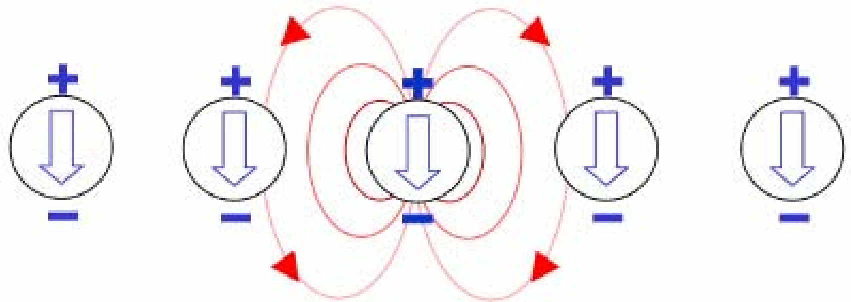

Interparticle coupling

Discrete dipole approximation

- Recognise that a ‘point scatterer’ acts like a dipole
- Replace with an array of dipoles on cubic lattice
- Solve for **E** field at every point dipole $\rightarrow$ know scattered field

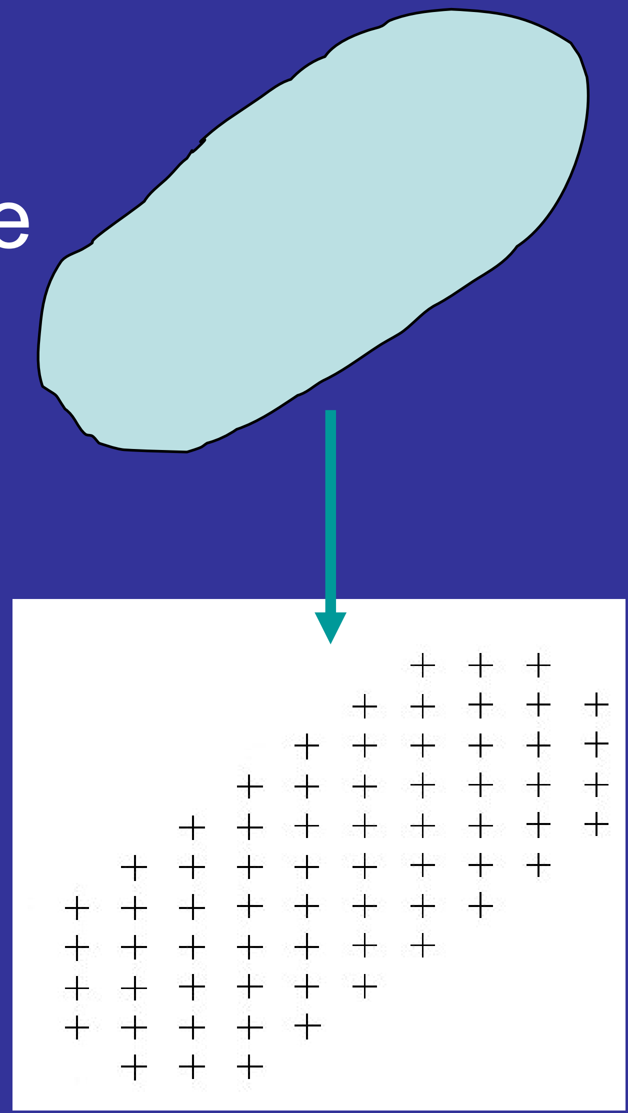

DDA simulation details

Neal, Palffy-Muhoray

- Discrete dipole approximation (DDA) simulation determines susceptibilites

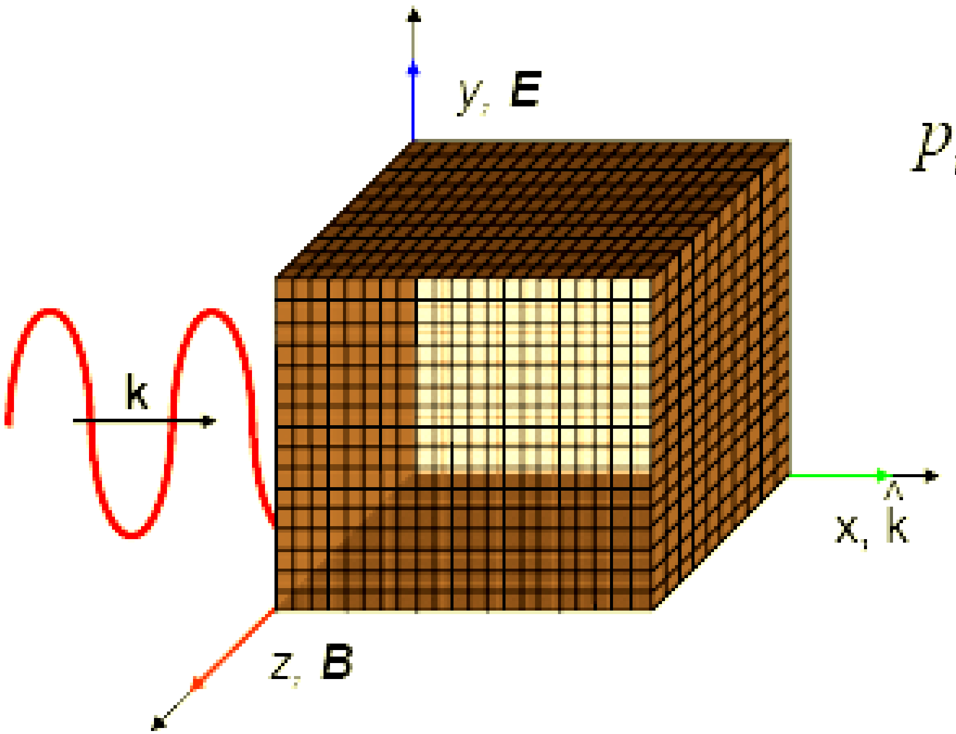

Simulation Solves:

$$p_i = \alpha_i (E_{inc,i} - \sum_{j \neq k}^{N} A_{jk} p_k)$$

If

$$\alpha_i^{-1} = A_{ii}$$

then

$$\sum_{i=1}^{N} A_{ij} p_i = E_{inc,j}$$

Results: computed dipole moments for Au NRs

Neal, Palffy-Muhoray

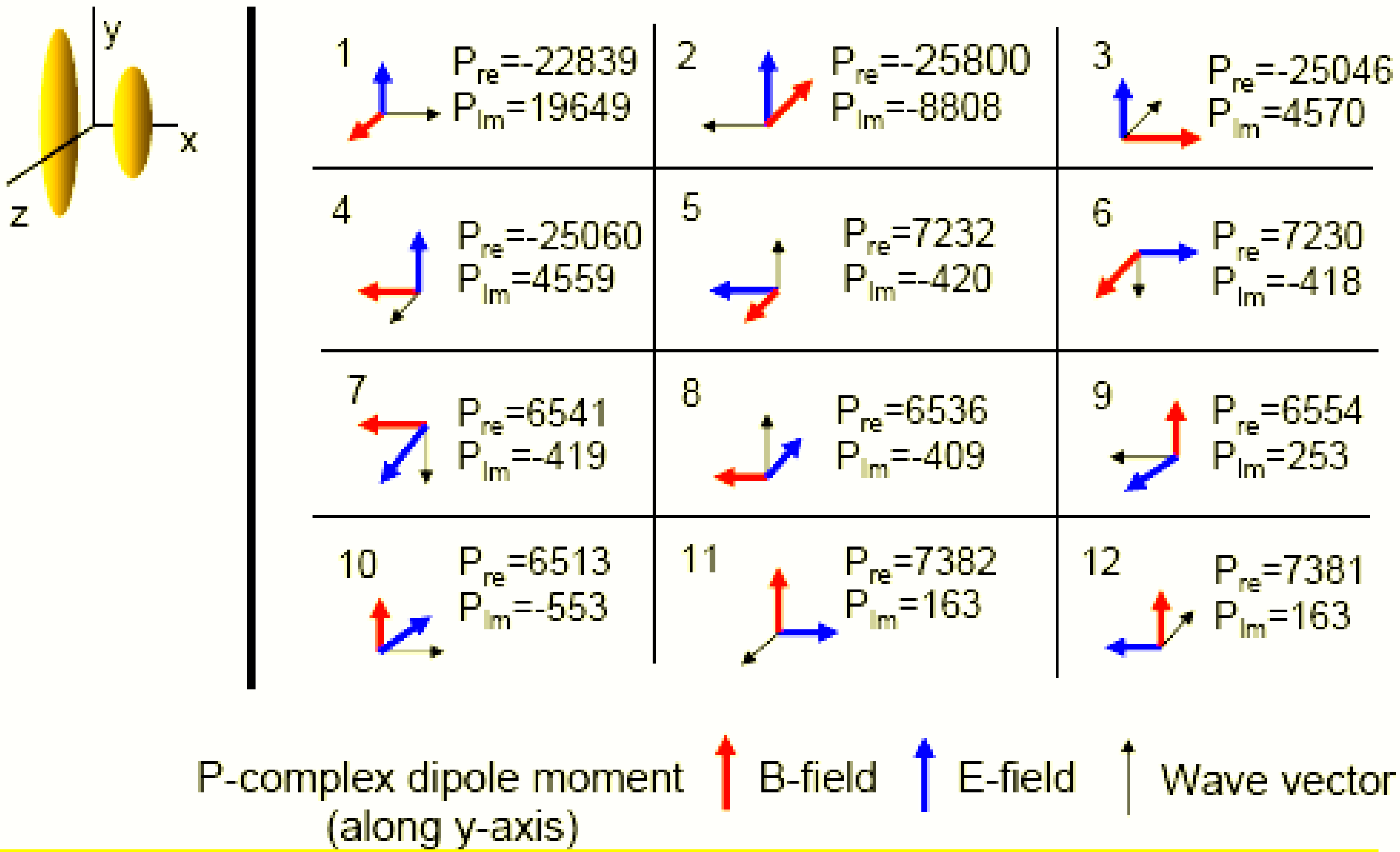

Discrete Dipole Approximation

- Consider N dipoles, the $i th$ dipole $\mathbf{p}_i$ located at $\mathbf{r}_i$ and having polarizability α_i.
- $\mathbf{p}_i = \alpha_i \mathbf{E}_{loc,i}$
- $\mathbf{E}_{loc,i} = \mathbf{E}_0 e^{\mathbf{k}\cdot\mathbf{r}-i\omega t} - \sum_{j\neq i} \mathbf{A}_{ij} \cdot \mathbf{p}_j$
- $\mathbf{A}_{ij} \cdot \mathbf{p}_j$ = dipole field (near-field + far-field contribution) at $\mathbf{r}_j$ due to $\mathbf{p}_i$.
- Solve for $\mathbf{p}_i$. Then extinction coefficient C_{ext} is given by

$$C_{ext} = \frac{4\pi k}{|\mathbf{E}_0|^2} \mathrm{Im} \sum_{\mathrm{j}=1}^{\mathrm{N_{par}}} \mathbf{E}_0^* \exp(-\mathrm{i}\omega \mathrm{t}) \cdot \mathbf{p}_\mathrm{j} \tag{1}$$

  by optical theorem. (N_{par} is the number of particles in the cluster.)

- α_i is related to ϵ_i of the i^{th} particle by requiring that it given the correct first scattering coefficient in the Mie expansion.

Refs. for DDA: E. M. Purcell and C. R. Pennypacker, Ap. J. **186**, 705 (1973); J. J. Goodman *et al*, Opt. Lett. **16**, 1198 (1991).

Discrete Dipole Approximation

- Purcell & Pennypacker, Ap. J. 186, 175 (1973); Goodman, Draine & Flatau, Opt. Lett. 16, 1198 (1991).
- Idea: break up small particle into small volumes, each of which carry dipole moment.
- Dipole moment due to local electric field from all the other dipoles.
- Calculate total cross-section, using multipole-scattering approach.
- Can be used for anisotropic, and absorbing, scatterers.
- Connect polarizability of small volume to dielectric function, using Clausius-Mossotti approximation

Discrete Dipole Approximation (DDA)

Standard method for determining the scattering properties of non axis-symmetric particles, completely flexible concerning target geometry

Approximation:

- Describe the actual target by an array of polarizable points (dipoles);
- Representation as electrical dipoles, magnetic dipoles and multipoles are neglected.

Required conditions:

- Best if targets have sizes comparable to wavelength (i.e. Mie-region)
- Materials should have $|m-1| < 1$ to 3, m = complex refractive index
- d: „interdipole separation" should be smaller than structural lengths and wavelength λ
- numerical studies indicate $|m|kd < 1$, $k=2\pi/\lambda$ (wave number)

DDA source code

- ✓ DDSCAT6.1 (Draine and Flatau, 2003), publicy available (GNU)
- ✓ FORTRAN (f77) software package (highly portable)
- ✓ Calculation of :
- ✓ - absorption, scattering, extinction efficiency factor
- ✓ - 4x4 Mueller scattering intensity matrix, amplitude scattering function
- ✓ Variables
- ✓ - target type/orientation (random/non-random)
- ✓ - scattering angles
- ✓ - number of dipoles
- ✓ - frequency, complex refractive index
- ✓ Size parameter (SP) < 15, |mkd| < 0.5

Validation of DDA

- DDA single scattering properties – comparison to Mie calculations
- DDA single scattering properties – comparison to T-matrix calculations

DDA single scattering properties – comparison to Mie calculations

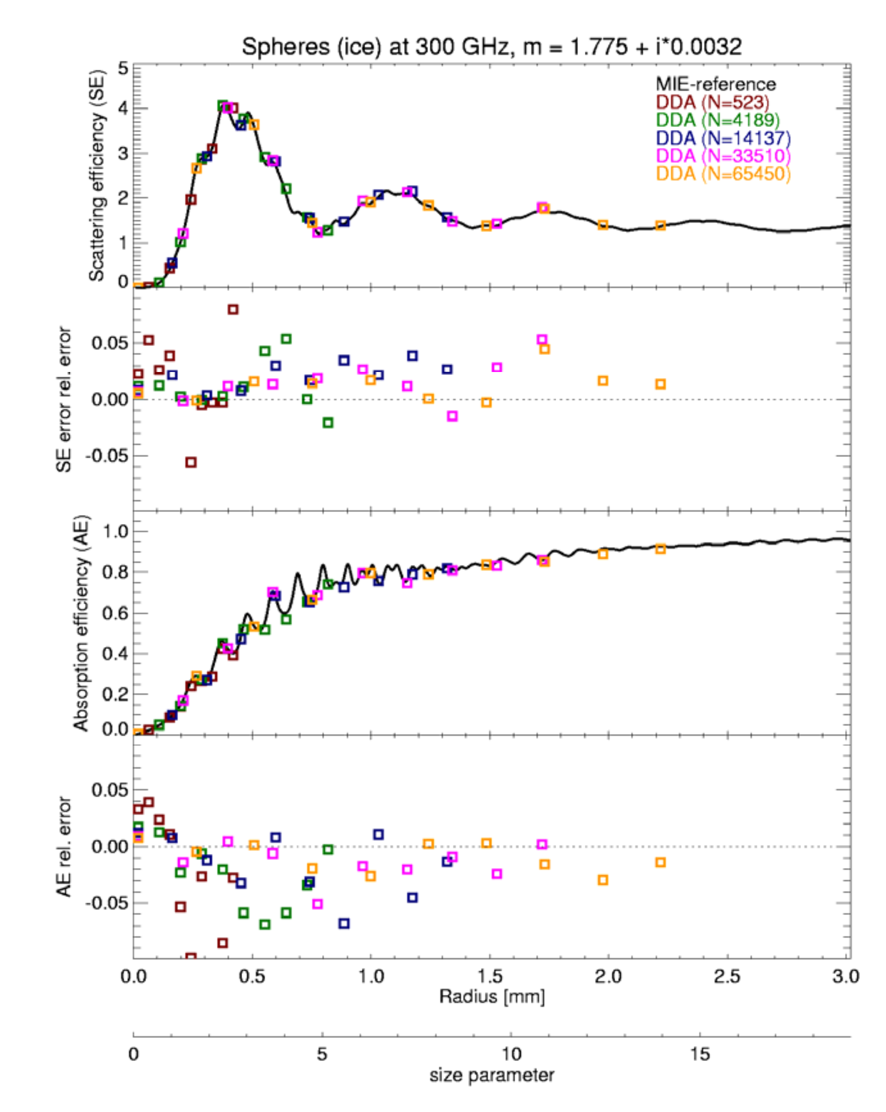

Solid ice spheres at 300 GHz

Criterion for DDA application:
mkd < 0.5
(see Draine and Flatau, 2003)

m: complex refractive index
k: wave number
d: dipole separation
N: number of dipoles

N ~ 1/d